The Dissertation Committee for Monte Alexander Kenaston certifies that this is the approved version of the following dissertation:

Investigation of the Physiological and Biochemical Function of Mitochondrial Uncoupling Protein 3

Committee:

_____
Edward M. Mills, Supervisor

_____
Shawn B. Bratton

_____
Andrea C. Gore

_____
Stephen D. Hursting

_____
Jon E. Sprague

Investigation of the Physiological and Biochemical Function of Mitochondrial Uncoupling Protein 3

by

Monte Alexander Kenaston, B.S.N., M.S.

Dissertation

Presented to the Faculty of the Graduate School of

The University of Texas at Austin

in Partial Fulfillment

of the Requirements

for the Degree of

Doctor of Philosophy

The University of Texas at Austin

December 2010

Dedication

I dedicate this dissertation to my father Monte R. Kenaston, PhD who has always supported my dreams and aspirations.

Acknowledgements

During the preceding five years, my mentor Dr. Edward (Ted) Mills has served as a guide, advisor, and confidant. Despite having little research experience, I was accepted as a student and Dr. Mills provided me with years of instruction, advice, and encouragement. My hope is that he views my tenure favorably and feels I have made a positive contribution towards the success of his laboratory. His enduring support and desire to encourage and instruct students has led to his success as a teacher and mentor.

I would like to thank my committee members for their service in guiding my doctoral research. Dr. Bratton was a constant presence and always provided me with helpful suggestions and advice. Dr. Gore has served as co-advisor for me and was essential in helping me apply for and receive a prestigious pre-doctoral fellowship. Despite working in another department Dr. Hursting readily agreed to serve on my committee and share his expertise and equipment. Lastly, Dr. Sprague was always available for consultation and graciously agreed to be on my committee despite living 1200 miles away.

I am extremely grateful for the friendships that were started in graduate school and forged through hours spent working at the laboratory together. Members of the Mills Laboratory (Matthew Pfeiffer, Katsuya Hirasaka, Sara Nowinski, Kristin Fathe, and Ellen Abramson) and Bratton Laboratory (Srinivas Malladi, Madhavi Malladi, Shankar Vardarajan, and Jae Kyoung Son) were great colleagues and friends to me throughout my time in graduate school.

I owe a great debt to the professionals that provided me with daily guidance, instruction, support, and friendship. A large part of my training was due to the capable, conscientious, and honorable Drs. Srinivas Malladi, Madhavi Malladi, and Katsuya Hirasaka. I have learned a great deal about life, marriage, respect, family, and science from these dear friends.

I would like to thank my mother Maria, father Monte, and brother Dale for their never-ending support of my personal and educational goals. They have remained interested and encouraging since my first day of graduate school. Finally, my wife Kristin has been my biggest supporter, always by my side, providing constant comfort and optimism. She and my daughter Alexa are the reasons I pursue advancement and personal betterment.

Investigation of the Physiological and Biochemical Function of Mitochondrial Uncoupling Protein 3

Monte Alexander Kenaston, Ph.D.

The University of Texas at Austin, 2010

Supervisor: Edward M. Mills

Uncoupling proteins (UCPs) are highly conserved inner mitochondrial membrane proteins that have been found in plants, nematodes, flies, and vertebrates. UCPs dissipate the proton gradient formed by the electron transport chain in an energy-expending process that generates heat. In mammals, the brown fat-specific UCP1 is thought to be the dominant, if not the only significant mediator of thermogenic responses. However, adult humans express only negligible amounts of brown fat and UCP1, yet still show significant non-shivering thermogenic responses (e.g. amphetamine-induced hyperthermia, diet induced thermogenesis, fever). Thus, the fact that human thermogenic mechanisms haven't been identified is a huge gap in our understanding of human thermoregulation.

UCP3 is primarily expressed in skeletal muscle, an established thermogenic organ which is a major target of amphetamine-induced pathology. UCP3 knockout mice have a near complete loss (~80%) of amphetamine-induced thermogenesis and are completely protected from amphetamine-induced death over a range of lethal doses. With regard to mechanisms of UCP3 activation, we observed that norepinephrine and free fatty acids are elevated in the bloodstream prior to peak amphetamine-induced hyperthermia. However,

little is known about the anatomic location of UCP3-dependent thermogenesis or the mechanisms by which fatty acids regulate UCP function. Thus, we sought to investigate the physiology and biochemical activation of UCP3 to establish the thermogenic potential of skeletal muscle uncoupling and elucidate the mechanisms of UCP3 function. The overall goal of this research was to identify the tissue target(s) and mechanisms involved in amphetamine-induced UCP3-dependent thermogenesis.

Herein, we show that in addition to a deficit in induced thermogenesis, UCP3-null mice also lack responses to other physiologically-relevant stimuli (i.e. catecholamines and bacterial pathogens). Conversely, UCP3 knockout mice, engineered to express UCP3 only in skeletal muscle have an augmented thermogenic response to amphetamines. In order to explore UCP3's mechanism of activation, we performed a modified yeast two-hybrid analysis and identified $\Delta^{3,5}\Delta^{2,4}$dienoyl-CoA isomerase (DCI) as a UCP3 binding partner. DCI, an auxiliary fatty acid oxidation enzyme, protects cells from the accumulation of toxic lipid metabolites. Using immunoprecipitation and fatty acid oxidation (FAO) assays, we determined that UCP3 and DCI directly bind in the mitochondrial matrix in order to augment lipid metabolism. These findings support a novel model in which skeletal muscle UCP3 is responsible for inducible thermogenesis through cooperation with binding partners such as DCI which enhance oxidation of fatty acids. Together, these studies shed light on thermogenic pathways in rodents that are likely to be relevant to humans.

Table of Contents

List of Figures

List of Abbreviations

ANT	Adenine nucleotide translocase
ATP	Adenosine triphosphate
BAT	Brown adipose tissue
BiFC	Bimolecular fluorescence complementation
BMI	Body mass index
BMR	Basal metabolic rate
β_3-AR	Beta adrenergic receptor, beta adrenoreceptor
β-ox	Beta oxidation
BSA	Bovine serum albumin
C16:0	Palmitic acid, palmitate
C18:1	Oleic acid, oleate
CAC	Carnitine/acylcarnitine carrier
CNS	Central nervous system
CO_2	Carbon dioxide
CoA	Coenzyme A
Cyt C	Cytochrome C
DAPI	Diamidino-2-phenylindole
DCI	$\Delta^{3,5}\Delta^{2,4}$dienoyl-CoA isomerase
DNA	Deoxyribonucleic acid
DNP	Dinitrophenol
DSP	Dithiobis[succinimidyl-propionate]
DxxK	aspartate-X-X-lysine
ECH	Enoyl Co-A hydratase
ECI	Enoyl Co-A isomerase
EDTA	2,2’,2”,2”’-(ethane-1,2-diyldinitrilo) tetraacetic acid
EGTA	Ethylene glycol tetraacetic acid
ETC	Electron transport chain

FA	Fatty acid
FAO	Fatty acid oxidation
FBS	Fetal bovine serum
FFA	Free fatty acid
GAPDH	Glyceraldehyde-3-phosphate dehydrogenase
GSIS	Glucose-stimulated insulin secretion
GST	Glutathione S-transferase
H^+	Proton
HBSS	Hank's buffered salt solution
HEPES	4-(2-hydroxyethyl)-1-piperazineethanesulfonic acid
HRT	Hormone replacement therapy
IPTG	isopropyl β-D-1-thiogalactopyranoside
IR	Insulin resistance
Kd	Kilodalton
MDMA	3,4-Methylenedioxymethamphetamine
METH	Methamphetamine
MR	Metabolic rate
mRNA	Messenger RNA
MTS	Mitochondrial targeting signal, mitochondrial targeting sequence
NaCl	Sodium chloride
NaOH	Sodium hydroxide
NE	Norepinephrine
NH_4Cl	Ammonium chloride
NP-40	Nonident P-40
O_2^-	Superoxide
OD	Optical density
PAGE	Polyacrylamide gel electrophoresis
PCR	Polymerase chain reaction
PMSF	Phenylmethylsulfonyl fluoride

PPAR	Peroxisome proliferator-activated receptor
PTS	Peroxisomal targeting signal, peroxisomal targeting sequence
PVDF	Polyvinylidene fluoride
qRT-PCR	Quantitative reverse transcriptase PCR
RIPA	Radioimmune precipitation assay buffer
RNA	Ribonucleic acid
RNAi	RNA interference
RPM	Revolutions per minute
SDS	Sodium dodecyl sulfate
SNS	Sympathetic nervous system
SKM	Skeletal muscle
T2DM	Type II diabetes mellitus, insulin-dependent diabetes mellitus
TCA	Tricarboxylic acid
TMRM	Tetramethyl rhodamine methyl ester
Tris-HCl	Tris(hydroxymethyl)aminomethane hydrochloride
UBI	Ubiquitous, ubiquitous expression
UCP	Uncoupling protein
V/V	Volume / volume
WAT	White adipose tissue
Ψ	Membrane potential

Chapter 1 – Introduction

1.1 Bioenergetics

All living beings must use energy to fuel biologic processes such as movement, metabolism, respiration, growth, and reproduction. The needs of the organism must be met through the procurement of energy from external food sources. It is the study of this flow of energy into, through, and subsequently out of an organism that is the field of bioenergetics (Campbell 2005). Animals, in particular, actively harvest their food from the environment to obtain chemical energy. Through digestion and metabolism, chemical energy is extracted from food and ultimately results in the production of adenosine triphosphate (ATP), a nucleotide that is perhaps the most important form of chemical energy currency in animals. ATP is used to fuel many cellular functions that all contribute to the survival of the organism and as such the production of ATP is intimately tied to organismal energy demands. Energy-consuming reactions produce heat as a consequence, thus the production of heat correlates to the metabolic rate of the animal.

The organelle principally responsible for meeting the energy demands of the cell is the mitochondrion. This bi-membranous organelle is the site of cellular respiration, a catabolic pathway that consumes oxygen in order to yield high-energy intermediates. The process of generating energy in the mitochondria is represented in the simplistic pathway in Figure 1.1. Substrates consumed as food are enzymatically degraded and transported into the cell and subsequently into the mitochondria. These substrates undergo metabolism prior to entering the TCA cycle (i.e. tricarboxylic acid cycle, citric

acid cycle, or Kreb's cycle) then intermediates subsequently contribute electrons to the electronc transport chain (ETC). The ETC is a group of membrane-associated proteins that accept and donate electrons in order to actively transport protons (H^+) from the mitochondrial matrix into the intermembrane space. This enforced concentration of protons across the inner mitochondrial membrane creates a membrane potential which is then used to fuel the F1/F0 ATP synthase protein that generates ATP from adenosine diphosphate (ADP). Thus, the ingestion and oxidation of substrates is coupled to the synthesis of ATP.

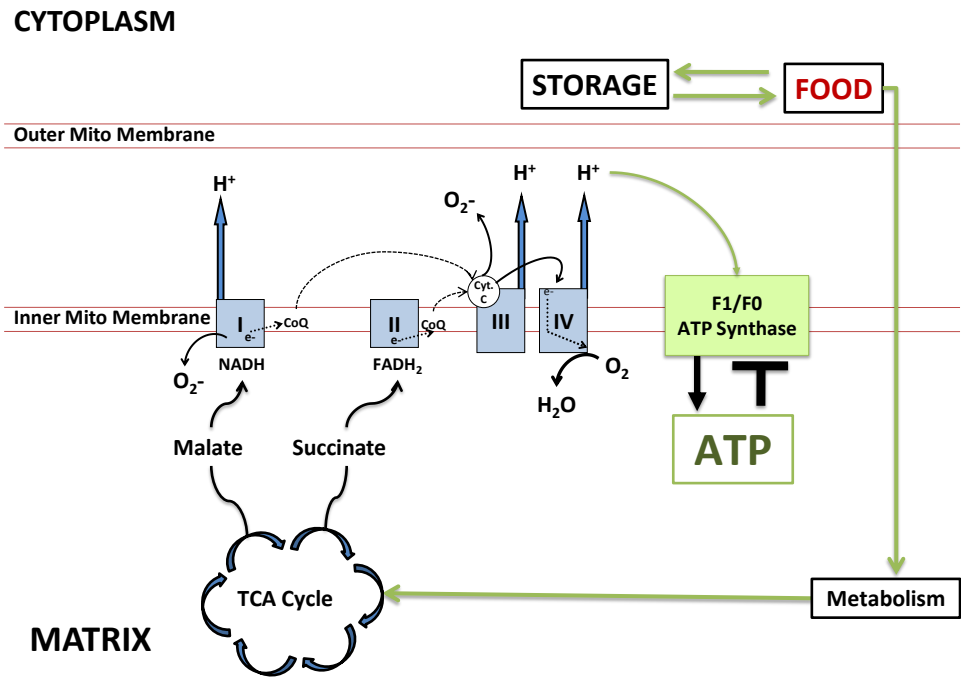

Figure 1.1 Mitochondrial Energy Production. Substrates ingested as food can either be stored or used for chemical energy. The mitochondrion represented in this figure is the primary site for energy generation for the cell. As substrates enter the mitochondrion, they undergo metabolism then enter the TCA cycle to produce intermediates (malate and succinate) which donate electrons to the ETC. The ETC pumps protons into the inner membrane space in order to create a proton gradient that is used to power the F1/F0 ATP synthase and generate ATP.

1.1.1 Metabolic Rate

In order to determine the energy needs of an organism, it is important to quantify the use of energy. A common principle in bioenergetics is the metabolic rate. This rate is the collective sum of energy required to perform all biologic processes over a unit of time. To some degree, the metabolic rate correlates well with the size of an organism with larger organisms having higher metabolic rates. The metabolic rate is an ever-fluctuating representation of an animal's current energy usage. In times of high metabolism, reproduction, or stress, this rate can increase substantially. However, the rate of energy use needed to power only the most basic life-support functions such as breathing and circulation is the basal metabolic rate (BMR). A living, active organism is never operating at its BMR, as any type of activity will consume excess energy. Thus, the metabolic rate is always in flux, increasing with energy demands, and being supplied by consumption of energy-producing materials. The body reacts to changing energy requirements through responsive feedback systems whose purpose is to achieve internal balance, a principle called 'homeostasis' (Campbell 2005).

1.1.2 Homeostasis

In an effort to achieve balance, homeostatic feedback mechanisms exist to respond to and resist changes in the internal environment. A parameter for the internal environment, such as body temperature, will have its own ideal setting or 'set point'. However, the constant flux of the internal environment means the set point is never achieved for long periods of time. Rather, there is always slight variation in the set point

as the body responds to changes imposed upon it by the activity of the organism, energy supply, and the external environment. Feedback loops exist to respond to changes in set points using receptors and effectors. Receptors serve to detect changes in internal environment, and then convey a message through the effectors in order to respond to the change. Positive feedback loops involve a receptor-effector activity that will respond to a change by increasing activity in the same direction as the observed change. Negative feedback loops, conversely, will prevent change in the same direction as the initial change detected by the receptor. Body temperature is a parameter of the internal environment that is regulated by a set point, receptor-effector relationships, and feedback loops.

Within the hypothalamic brain region there are a collection of nerve cells which function as a thermostat for the maintenance of internal body temperature. These nerve cells participate in the positive and negative thermoregulatory feedback loops. Temperature-sensing nerve cells are present throughout the body, with high concentrations being found in the skin. In an example of positive feedback, nerve receptors in skin may detect increasing body temperature which will cause effectors (e.g. sweat glands) to increase their cooling of the body. In an example of negative feedback, the same receptors that sense rising temperatures may trigger other effectors (e.g. vascular smooth muscle) to prevent peripheral vessel dilation.

Animal species employ different strategies to perform the maintenance of body temperature. Ectotherms, such as fish, reptiles, and amphibians utilize the external environment to maintain their internal body temperature. The metabolic requirements of

an ectotherm are relatively low, and as a consequence they have a low metabolic rate. In contrast, the endotherms, which are primarily mammals and birds, rely on internal mechanisms. Endotherms have a high metabolic rate and are able to regulate their internal body temperature to a precise degree. This tight regulation comes at an expensive cost energetically, however, and as a substantial benefit endotherms are capable of operating in ambient temperatures substantially different from their internal set point. These two metabolic strategies are used to control internal body temperatures through behavior, anatomy, and physiologic responses in a process called 'thermoregulation'. While thermoregulation by ectotherms is primarily evidenced through changes in their behavior (i.e. locating areas of different ambient temperature, feeding), the endothermic strategy is much more complex.

1.1.3 Thermoregulation

Thermoregulation is the process by which animals maintain temperature homeostasis. Endotherms perform this function by using anatomical (i.e. insulation, circulation) and biochemical (i.e. evaporation, heat production) means to balance heat loss versus heat gain (Campbell 2005). The integument of mammals and birds provides insulation from ambient temperatures and is extremely effective at controlling the loss of heat through the skin. In addition, adipose tissue immediately beneath the skin can augment this protection. Some animals also have fur or feathers to provide further insulation against the external environment. The circulatory system carries nutrient-rich blood to distant tissues. This transport function is also utilized in thermoregulation to

either cool (i.e. shunting blood away from the core) or heat (i.e. shunting blood to the core) the body through the movement of blood. Biochemical processes are also utilized by endotherms to maintain temperature homeostasis. Because water absorbs heat when it evaporates, saliva and the production of sweat are used for evaporative heat loss. Finally, organisms can also employ metabolic heat production, also known as 'thermogenesis.'

1.2 Thermogenesis

The regulation of core body temperature is a tightly-controlled process that is proposed to be governed by the hypothalamic-pituitary-thyroid (HPT) axis and the sympathetic nervous system (SNS) (Sprague, Banks et al. 2003). Although all of the molecular mediators of thermogenesis still remain to be identified, several have been proposed including adrenergic receptors and mitochondrial uncoupling proteins (UCPs). Traditional thermogenesis, or non-shivering thermogenesis, is a normal physiological process. In rodents, a major contributor to non-shivering thermogenesis is uncoupling protein 1 (UCP1) which is present in brown adipose tissue (BAT). Humans, however, have negligible amounts of BAT or UCP1 but still have the capacity for non-shivering thermogenesis. Other uncoupling protein homologs such as UCP3 (found in skeletal and heart muscle) may be responsible for this effect, although this is a matter of intense scientific debate. In addition to rapid temperature-adjusting responses such as non-shivering thermogenesis, the concepts of body temperature regulation and energy expenditure are intimately related to homeostasis.

A current focus of intense research in the realm of obesity and weight loss is adaptive thermogenesis. The expenditure of energy as heat (thermogenesis) can be studied in carefully controlled trials that examine the subject's change in weight versus their energy intake. Several researchers have found that dramatic changes in diet often do not lead to dramatic changes in fat content or weight, purportedly due to adaptive thermogenesis (Major, Doucet et al. 2007). This adaptation to a dramatic change in substrate availability can lead to no effect or a paradoxical effect upon body weight and fat composition. The theory of adaptive thermogenesis is that the body has the capacity to regulate energy expenditure under normal physical conditions. Drastic changes in energy intake, such as during dieting or starvation, do not always have the anticipated effect (loss of fat reserves) due to the stabilizing effect of adaptive thermogenesis. This is proposed to be a significant obstacle to obesity treatments and weight loss regimens (Major, Doucet et al. 2007).

Although traditionally thermogenesis is thought of as the ability to produce heat, it is perhaps more appropriate to consider it as the ability to regulate the core body temperature (Campbell 2005). In addition to raising body temperature, there are several examples of animals that prevent thermogenesis to survive adverse conditions by *lowering* core body temperature. This phenomenon that occurs in rodents, marsupials, and small mammals is known as hibernation. Hibernation is characterized by a shift in substrate utilization from predominantly carbohydrate to entirely lipid (i.e. fat stores) (Andrews 2007). This dramatic shift is thought to be induced at least partly by environmental factors such as cold temperatures, scarcity of food, and shortening

daylight hours. Although induction of hibernation may have environmental influence, widespread molecular differences have been observed in animals in torpid versus active states. Like other forms of thermoregulation, hibernation is thought to also be controlled by the master regulator thyroid hormone (TH). Circulating thyroid hormone levels are thought to drop due to an increase in the serum level of thyroxine binding globulin (TBG) (Andrews 2007). Thyroid hormone has also been proposed to play an important role in mediating the hyperthermic responses in various heat illnesses including amphetamine-induced pathologic hyperthermia (Sprague, Banks et al. 2003).

1.2.1 Hyperthermia and Heat Illnesses

As discussed previously, thermoregulation is a well-controlled process that has the capacity to adapt either rapidly (e.g. muscle movement or hormone release) or transcriptionally (i.e. gene expression of proteins) to alter the metabolic state and maintain homeostasis. Fever is perhaps the most common heat-related symptom that occurs under this tight control. Fever is a common response to the presence of pathogens or to endogenous systemic inflammation. Fever is defined as an elevated body temperature beyond the range considered normal (usually 39.3°C). In general, fever is viewed as a negative clinical finding although it reportedly is beneficial for the host immune response (Aiyagari and Diringer 2007). Aberrations in the regulation of this process can lead to core body temperatures in excess of 104°F that can lead to seizures and neurological deficits.

Some pathologically altered states can lead to more severe heat-related illnesses such as heat stroke and malignant hyperthermia. Heat stroke is usually caused by an inability to dissipate heat that is being produced in the body. This may occur by physical exertion in a warm climate, or even without strenuous exercise (Jardine 2007). Malignant hyperthermia, conversely, usually occurs in response to pharmacological triggers in a genetically-susceptible individual. Affected individuals usually have mutations of the ryanodine receptor that is present in smooth endoplasmic reticulum (Jardine 2007). In this illness, excessive futile calcium cycling in the sarcoplasm of skeletal muscle generates heat, much in the same way "futile" mitochondrial proton flux generates heat – energy that is released from ion flux, but not consumed – and is given off as heat. Dantrolene inhibits the ryanodine receptor and is the established treatment for malignant hyperthermia (Blank and Boggs 1993). Both of these conditions are easily treated with either removal of the heat stimulus or administration of dantrolene, respectively. A unique and less treatable type of hyperthermia emerges in response to toxic doses of amphetamines, such as methamphetamine and MDMA.

1.2.2 Investigational Models of Thermogenesis

The study of thermogenic mechanisms in animals demands the need to employ models that mimic naturally-occurring, physiologic phenomena. Currently, the most utilized investigational models are diet-induction, cold exposure, and adrenergic stimulation. Although these models represent distinct methods, they all intersect at downstream pathways of thermogenesis. The concept of diet-induced thermogenesis was

first realized when rats fed a high-fat, high-sugar diet (i.e. “cafeteria diet”) failed to increase their body weight consistent with their caloric intake (Rothwell and Stock 1979). This lack of weight gain has been attributed to adaptive thermogenesis by specific tissues. The pre-feeding of cafeteria style foods has routinely been employed to study diet-induced thermogenesis, although this phenomenon has recently been challenged (Kozak 2010). The exposure of a laboratory animal to cold environments has been used extensively to study adaptive mechanisms (Roberts and Smith 1967). This method was first described during the study of hibernation (Smith and Hock 1963). Lastly, the administration of amphetamines or drugs that cause release of endogenous adrenergics (i.e. catecholamines such as norepinephrine, epinephrine, and dopamine) has been used for thermogenic studies. Norepinephrine administration was used in pivotal experiments to show that cold-acclimated mice shunt blood to target organs to increase heat (Foster and Frydman 1978). Amphetamines can be viewed as ‘effectors’ downstream of both hi-fat feeding and cold-exposure.

1.2.3 Brown Adipose Tissue

Brown adipose tissue (BAT) is a well-circumscribed tissue present in several peripherally-distributed depots (e.g. intraspacular, cervical, perirenal, periaortic). The intrascapular depot is the largest single collection, accounting for approximately 25% of all BAT (Smith and Horwitz 1969). In contrast to white adipose tissue (WAT), which is primarily a storage reservoir for fatty acids, the BAT tissue morphology suggests a more active function. Using electron microscopy, BAT has been observed to contain many

mitochondria, indicating that it is an energetically demanding tissue (Smith and Horwitz 1969).

The theory that BAT was thermogenic first began when it was observed to undergo changes in morphology (i.e. hypertrophy, hypervascularization, engorgement) when exposed to cold temperatures (Smith and Horwitz 1969). Later it was established that blood flow was specifically increased to BAT after cold exposure (Foster and Frydman 1978). Subsequently, it was speculated that the prominence of BAT in newborn mammals evolved as a protective measure to counteract low ambient temperatures (Casteilla, Champigny et al. 1989). Thus, its role in the maintenance of body temperature was speculated although its utility was thought to be important for very specific scenarios; 1) in neonates for nonshivering thermogenesis, 2) after cold exposure to stabilize body temperatures, or 3) to facilitate arousal of the hibernating animal (Smith and Horwitz 1969). Recent evidence suggest that BAT exists in humans even independently of the scenarios mentioned above (Nedergaard, Bengtsson et al. 2007; Zingaretti, Crosta et al. 2009). However, the prevalence in the general population and the significance of its existence still remains to be established.

1.2.4 Thermogenin, the First UCP

Although BAT was well-described as a thermogenic tissue which responds to cold-acclimation (Foster and Frydman 1978), the mechanism responsible for this effect was initially unknown. As other groups clearly showed a proliferation of mitochondria in BAT (Smith and Horwitz 1969), research into the mechanisms of thermogenesis focused

on this organelle. Isolated mitochondria from BAT exhibited a pattern of uncontrolled respiration that appeared to be in excess of that required to meet the energy demands of the cell (Hittelman, Lindberg et al. 1969; Rafael, Ludolph et al. 1969). This research showed that the respiration could be inhibited by adding purine nucleotides or fatty acid-sequestering bovine serum albumin (Rafael, Ludolph et al. 1969). Later it was discovered that radiolabeled nucleotides associated with the outer surface of the inner mitochondrial membrane (Nicholls 1976). Based upon these data, Nicholls and colleagues concluded that a protein present on the inner mitochondrial membrane was responsible for the high respiratory capacity of BAT mitochondria. Using a technique referred to as photoaffinity labeling, the molecule was identified as a 32 kilodalton protein which accounted for approximately 10% of total mitochondrial protein content (Nicholls 1976). This protein was uncoupling protein 1 (UCP1), the archetypical uncoupling protein, also called thermogenin.

UCP1 is by far the most well-studied of the UCP family and the numerous investigations performed since its discovery have yielded significant insight into its structure, function, and contribution to mammalian physiology. All uncoupling proteins are members of the SLC25 solute carrier family of proteins that share a similar structure (Figure 1.2). These proteins are integrated into the inner mitochondrial membrane that separates the mitochondrial matrix from the intermembrane space. UCP1 has been shown to dissipate the proton gradient across the mitochondrial inner membrane. By increasing the proton conductance of the membrane, energy is wasted as heat (Cannon and Nedergaard 2004). The activity of UCP1 is inhibited at physiological levels of

purine nucleotides (i.e. adenosine phosphates, guanosine phosphates). This inhibition is quickly released as the protein encounters an increasing concentration of fatty acids in the mitochondrial matrix. Simply stated, the activation of an uncoupling protein consumes energy and generates heat (Figure 1.3).

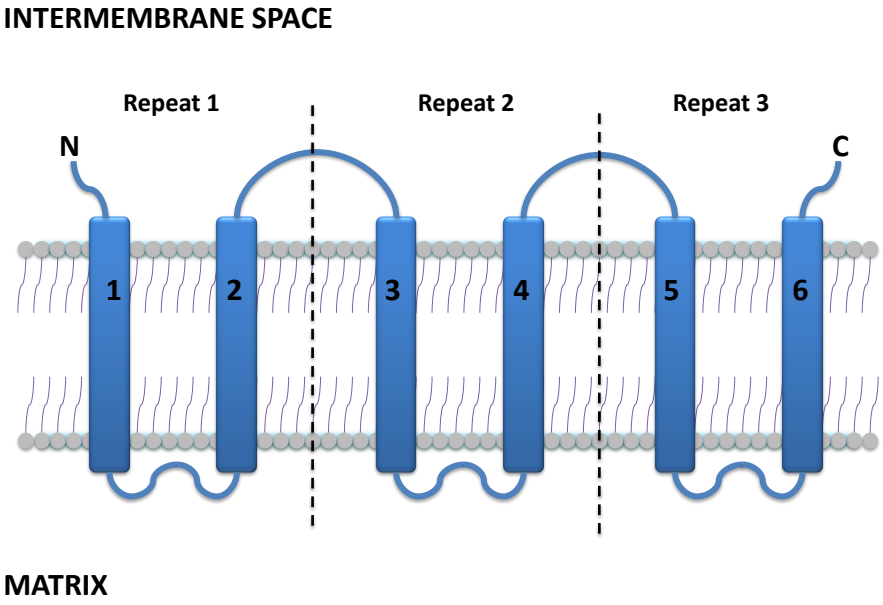

Figure 1.2 The SLC25 Solute Carrier Mitochondrial Proteins. This family of inner mitochondrial membrane proteins transport molecules between the mitochondrial matrix and the intermembrane space. Three tandem repeats each have two transmembrane domains and both the N and C termini localize to the intermembrane space.

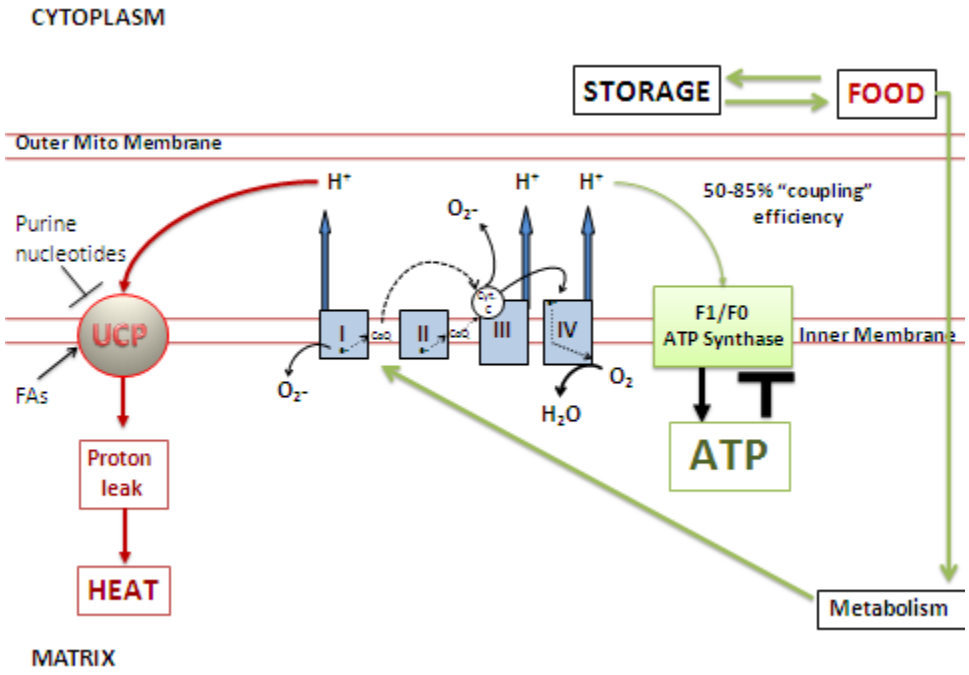

Figure 1.3 Uncoupling Protein Function. As the electron transport chain (ETC) generates the proton gradient necessary to power the synthesis of ATP, uncoupling proteins can intervene to "uncouple" this system. Protons used to form the gradient in the inner membrane space are transported back into the mitochondrial matrix by UCP in a reaction that gives off heat. The metabolism of substrates increases, as does the consumption of oxygen.

1.2.5 Uncoupling Protein Homologues

The uncoupling proteins are a subset of the mitochondrial solute carrier family of proteins. Since the discovery of UCP1 in 1976, other homologues have been identified based upon their protein sequences (UCP1-5) (Figure 1.4). Whereas UCP1 is expressed solely in BAT, other UCPs have distinct tissue expression patterns. UCP2 was originally identified in 1997 and is ubiquitously expressed (Fleury, Neverova et al. 1997). UCP3, also identified in 1997, is primarily expressed in skeletal muscle and to a lesser degree in heart and BAT (Vidal-Puig, Solanes et al. 1997; Boss, Giacobino et al. 1998). Initial excitement that these proteins would behave in a manner similar to UCP1 arose from the analysis of conserved domains purported to be important for proton conductance and nucleotide binding. Relatively little is known about the most recent UCP family members, UCP4 and UCP5. UCP4 is expressed in virtually all areas of the brain and spinal cord (Mao, Yu et al. 1999). UCP5, also known as BMCP1, is expressed in specific brain regions such as the cortex, hippocampus, and thalamus (Kim-Han, Reichert et al. 2001). Both UCP4 and UCP5 share low sequence homology with UCP1, and more closely resemble the dicarboxylate carrier, another mitochondrial protein (Palmieri 2004).

PROTEIN	% IDENTITY	RESIDUE OVERLAP	TISSUE EXPRESSION
UCP1	100%	307	BAT
UCP2	59%	300	UBI
UCP3	57%	311	SKM,HRT,BAT
UCP4	30%	294	CNS
UCP5	33%	282	CNS

Figure 1.4 The Uncoupling Protein Homologs. The prototypical uncoupling protein 1 (UCP1) was the first identified in brown adipose tissue (BAT). Subsequently UCP2 (UBI, ubiquitous expression) and UCP3 were discovered (SKM, skeletal muscle; HRT, heart; BAT). Both UCP4 and UCP5 have only ~30% homology with UCP1 andtheir expression is limited to the central nervous system.k

1.2.6 Uncoupling Protein 3

As mentioned above, the UCP1 homolog UCP3 was discovered in 1997. Its characterization revealed that it is present in specific tissues, in contrast to the ubiquitous expression pattern of UCP2 (Boss, Samec et al. 1997). This was of particular interest because it was found mainly in established thermogenic organs, skeletal muscle, brown adipose tissue, and heart (Boss, Samec et al. 1997). Initial studies supported a role for UCP3 in thermogenesis because it was found to be upregulated in response to cold-exposure in a manner similar to UCP1 (Larkin, Mull et al. 1997). However, subsequent investigations concluded that mice genetically engineered to lack UCP3 had no deficit in body temperature regulation, notably in response to cold (Golozoubova, Hohtola et al. 2001). Thus, the actual function of UCP3 has been a source of controversy. No definitive physiologic or biochemical function for UCP3 has been established.

1.3 Physiological Functions of Uncoupling Protein 3

Previous studies have provided conflicting hypotheses on whether UCP3 is a thermogenic protein (Larkin, Mull et al. 1997; Golozoubova, Hohtola et al. 2001). In addition, some groups have reported that the upregulation of UCP3 during fasting (Samec, Seydoux et al. 1998; Cadenas, Buckingham et al. 1999; Gong, Monemdjou et al. 2000) is not congruent with the energy-wasting consequence of UCP3 activation (Azzu, Jastroch et al. 2010). Another piece of evidence to refute a role for UCP3 in adaptive thermogenesis is the presence of its homologues in fish (Stuart, Harper et al. 1999) and plants (Laloi, Klein et al. 1997). Both fish and plants are ectotherms which are generally

thought to not possess the capacity for adaptive thermogenesis, although recent examples of uncoupling protein function in plants refute this (Smith, Ratcliffe et al. 2004; Ito-Inaba, Hida et al. 2008). Finally, what is regarded as the most definitive study on the lack of UCP3's thermogenic potential showed that UCP3 knockout mice retain the capacity for nonshivering, adaptive thermogenesis in response to cold (Vidal-Puig, Grujic et al. 2000). However, some evidence does exist to support the integration of UCP3 into existing thermoregulatory pathways.

The Djungarian hamster, which specifically lacks UCP3 in BAT, was found to have a defect in cold-tolerance despite the presence of active, functional UCP1 (Nau, Fromme et al. 2008). The interpretation of these results is difficult as this model has not been employed for the majority of other studies on the function of UCP1 and UCP3. Also, the UCP3 deletion in the Djungarian hamster is caused by missense mutation, rather than a genetically engineered knockout. Thus, the replication of these studies in traditional inbred mouse strains is needed. Another important and socially-relevant finding of UCP3 function arose from studies of the amphetamine compound 3,4-methylenedioxymethamphetamine (Ecstasy, MDMA). A principal observation in the toxicity evoked by MDMA and related amphetamines is an inability to regulate body temperature subsequently leading to life-threatening hyperthermia and death. Mice lacking UCP3 had a blunted thermogenic response to MDMA and were completely protected from death after MDMA administration (Mills, Banks et al. 2003).

The studies performed to date to investigate the physiologic function of UCP3 have left several unanswered questions. Previous reports on the thermogenic potential of

UCP3 have utilized the cold-exposure model to suggest that UCP3 is not required for adaptive thermogenesis (Vidal-Puig, Grujic et al. 2000; Golozoubova, Hohtola et al. 2001). In these investigations, mice lacking UCP3 were subjected to cold ambient temperatures and they were able to mount a thermogenic response sufficient to maintain internal temperatures at a constant level. These studies provide important evidence that UCP3 is not required for cold-induced thermogenesis but do not address the role of UCP3 in responding to other stimuli. These studies also ignore the established role of UCP1 in thermogenesis and do not test for UCP3 effects. In modern society, the thermogenic response to dangerously cold ambient temperatures is perhaps a scenario that is less meaningful to the human population than other more physiologically-relevant triggers (i.e. pathogen-induced fever, endogenous catecholamine release).

The most definitive study showing a positive UCP3-dependent thermogenic effect illustrated that amphetamines are perhaps the most potent stimuli (Mills, Banks et al. 2003). Although this report provides clear evidence for the involvement of UCP3 in amphetamine-induced thermogenesis, the organ responsible has not been identified. UCP3 is expressed primarily in skeletal muscle, heart, and to a lesser degree in BAT (Boss, Samec et al. 1997). Because previous reports have shown that BAT function (i.e. nonshivering, adaptive thermogenesis) is not negatively affected in a UCP3 knockout animal, it is important to differentiate the organ responsible for the strong amphetamine-induced toxicity phenotype (i.e. rule out or provide evidence for skeletal muscle UCP3 as the effector organ).

1.4 Biochemical Functions of Uncoupling Protein 3

The biochemical functions of UCP3 have been explored in numerous previous studies. It has been proposed to function in relieving oxidative stress, protecting against insulin resistance, and increasing fatty acid oxidation. Very few conclusive findings have been accepted by the scientific community. The majority of work on UCP3 function has been devoted to the mitigation of reactive oxygen species (ROS). ROS form when availability of substrates exceeds energy demands. These dangerous by-products can attack cellular proteins, DNA, and lipids leading to dysfunction or cell death. Evidence for the capacity of UCP3 to deal with high ROS levels comes from studies that show UCP3 is activated by endogenous (Talbot, Hanuise et al. 2003; Talbot, Lambert et al. 2004) as well as exogenous ROS (Echtay, Roussel et al. 2002), and lipid peroxides (Murphy, Echtay et al. 2003). *In vivo* models have illustrated that UCP3 decreases ROS-induced protein damage in skeletal muscle (Barreiro, Garcia-Martinez et al. 2009) and may act during times of high ROS levels such as exercise (Jiang, Zhang et al. 2009).

Another proposed biochemical function of UCP3 is the amelioration of insulin resistance. This theoretical action is of great interest in light of the tremendous societal burden currently ongoing as a result of obesity and Type 2 diabetes mellitus (T2DM). Insulin resistance in skeletal muscle is the major cause of T2DM (Chan and Harper 2006). Evidence for this protection conferred by UCP3 comes from studies which show that mice overexpressing UCP3 (specifically in skeletal muscle) are protected from obesity and insulin resistance (Son, Hosoda et al. 2004). Current standard of care treatment for T2DM involves the use of PPAR agonists to treat insulin resistance. Insulin

resistance is a physiologic phenomenon during which the natural protein insulin becomes less effective at eliciting the import and metabolism of glucose and fatty acids. The efficacy of this treatment may be explained by the upregulation of UCP3 by PPAR treatment in diabetic patients (Schrauwen, Mensink et al. 2006).

Lastly, a role for UCP3 in fatty acid metabolism has been investigated. Some groups have argued that UCP3 may act as a fatty acid transporter (Himms-Hagen and Harper 1999; Himms-Hagen and Harper 2001; Schrauwen, Hoeks et al. 2006) while others have contested this notion (Seifert, Bezaire et al. 2008). Work performed in mice with UCP3 overexpressed specifically in skeletal muscle have shown an increase in fatty acid transport and oxidation (Bezaire, Spriet et al. 2005). Likewise others have shown increased fatty acid oxidation during fasting was UCP3-dependent (Seifert, Bezaire et al. 2008). The capacity for UCP3 to increase oxidation/metabolism of fatty acids is of particular importance given the global epidemic of obesity. This potential function should be further explored to determine the therapeutic possibilities for targeting relevant human diseases.

1.5 Concluding Remarks

The energy demands of an organism are determined by its size, activity, environment, and physiology. The maintenance of body heat, as in endotherms, is an energetically costly process. In order to maintain vital functions such as cell maintenance, breathing, and circulation, an organism must achieve its BMR. The BMR is the sum of all energy required to perform necessary cellular processes while the

organism is at rest. The ability of an organism to exceed this basal metabolic rate in times of greater energetic needs varies substantially, but ultimately depends on the availability of substrates. The mitochondria are the organelles which are principally responsible for the generation of ATP, the high-energy intermediates used to fuel the majority of cellular operations. ATP is generated via the mitochondrial membrane electron transport chain and oxidative phosphorylation (Figure 1.1). The generation of ATP relies on the consumption of substrates (i.e. food), however this process is not 100% efficient. The mitochondrial uncoupling proteins (UCPs) are inner membrane proteins that can interfere with or uncouple the generation of ATP by dissipating the proton gradient that fuels ATP synthesis (Figure 1.3). This process promotes a rapid increase in oxygen consumption and wastes substrate oxidation as heat. Thus, the activation of uncoupling proteins results in heat production, energy-wasting, and increased metabolism of substrates.

The generation of heat, or thermogenesis, is a crucial physiologic characteristic of endotherms. The mediation of adaptive thermogenesis in BAT by the archetypal UCP1 is well-established. Other UCP1 homologs, such as UCP3, are still in need of further investigation. Previous studies have shown that UCP3 is primarily expressed in skeletal muscle (Larkin, Mull et al. 1997; Vidal-Puig, Solanes et al. 1997) and does not have the same function as UCP1 (Vidal-Puig, Grujic et al. 2000). However, UCP3 may still be important for other types of thermogenesis such as under different experimental conditions or with different stimuli. Other possible roles for UCP3 include the mitigation

of reactive oxygen species, the protection from insulin resistance, or the augmentation of fatty acid transport or oxidation.

Two main gaps in our understanding of UCP3 function and activity exist. From an anatomical and physiological standpoint, the only clear UCP3-dependent phenotypical observation has been observed in response to amphetamines (Mills, Banks et al. 2003). UCP3 knockout animals lose the hyperthermic response to amphetamines that is seen in wild type animals. However, UCP3 is expressed in brown fat as well as skeletal muscle, both established thermogenic organs. This investigation will attempt to address the contribution of UCP3 in BAT versus skeletal muscle to the amphetamine-induced thermogenic phenotype. Although many studies have been performed exploring UCP3 function, none have proposed a mechanism that involves intimate cooperation with other proteins. Another goal of this investigation was to study the mechanism of proposed UCP3 functions through the interrogation of protein-protein interactions. Collectively, the data shown in this investigation will contribute to the understanding of UCP3 function and its role in metabolism.

Chapter 2 – Methods and materials

2.1 Chemicals and Reagents

Unless otherwise stated, all reagents and chemicals were obtained from Sigma-Aldrich (St. Louis, MO).

2.2 Yeast Two Hybrid

This screening was performed according to the method of Pierrat et al. (Pierrat, Ito et al. 2000). The seven hydrophilic loop regions of mouse UCP3 were cloned into a pGBKT7 vector containing the GAL4 DNA binding domain which was used as bait against a human heart cDNA library.

2.3 Plasmid DNA Constructs

Full length mUCP3 and mDCI were amplififed from a mouse heart cDNA library. These fragments were cloned into a pcDNA3.1 vector with V5 tag or pcDNA6 vector with myc or GFP tag, respectively (Invitrogen, Carlsbad, CA).

2.4 Cell Culture

HeLa, C2C12, H9C2, FVBC3, and NIH3T3L1 cells were obtained from the American Type Culture Collection (ATCC, Manassas, VA). All cells were cultured in Dulbecco's Modified Eagle Medium containing 10% FBS and 1% 100X PenG-Streoptomycin (Invitrogen, Carlsbad, CA) with 5% CO_2 at 37°C. Transient transfections

were performed using either Fugene HD reagent (Roche Applied Sciences, Indianapolis, IN) or Lipofectamine (Invitrogen, Carlsbad, CA) per the manufacturer's instructions. Cells were incubated for 24 or 48 hours prior to treatments or experiments.

2.5 Immunoblotting

Cell or tissue lysates were prepared in RIPA buffer (50mM Tris-HCl, 1% NP-40, 0.5% Sodium Deoxycholate, 0.1% SDS, 150mM NaCl, 2mM EDTA, pH 8.0). The Pierce bicinchoninic acid assay (Pierce Biotechnology, Rockford, IL) was used for protein quantitation. Samples were then prepared for SDS-PAGE with 4X sample (250mM Tris-HCl, 8% SDS, 40% glycerol, 8% β-mercaptoethanol, 0.02% bromophenol blue) and separated on 10 or 12% gels. Proteins were then transferred to nitrocellulose or PVDF membranes and probed with primary antibodies per the manufacturer's instructions; mouse monoclonal anti-myc (Cell Signaling, Danvers, MA), rabbit polyclonal anti-V5 (Abcam, Cambridge, MA), mouse monoclonal anti-GFP (Invitrogen, Carlsbad, CA), ADRB3 goat polyclonal (Santa Cruz Biotechnology, Santa Cruz, CA). Custom antibodies were generated for mUCP3 and mDCI (Washington Biotechnology, Columbia, MD) and used at a concentration of 1:500 in 5% milk for 16 hours at 4°C. Secondary antibodies were sheep anti-mouse and donkey anti-rabbit (Amersham, Pescataway, NJ) or donkey anti-goat (Santa Cruz Biotechnology, Santa Cruz, CA). Membranes were then developed using Super Signal West Pico or Super Signal West Femto chemiluminescent (Pierce Biotechnology, Rockford, IL).

2.6 Immunoprecipitation

Protein lysates of 100µg were prepared in 300 µL of immunoprecipitation buffer (RIPA or 1% Triton X-100 in PBS). Samples were incubated with either 2µg of primary antibody or IgG for controls at 4°C for 16 hours with rotation. Protein A/G Sepharose beads (30µL) were added to each sample and then rotated for 4 hours at 4°C. Beads were then washed in high-stringency immunoprecipitation buffer (1% Triton X-100 in PBS or RIPA with 600mM NaCl) and prepared for SDS-PAGE as described above. For samples that were cross-linked, we used the method of Thompson et al. (Thompson and Kim 2004) with the following modifications; the plasma membrane permeable crosslinker DSP (Pierce Biotechnology, Rockford, IL) was applied to cells at a concentration of 1mM per manufacturer's instructions. The crosslinking reaction was stopped with the stop buffer (1M Tris, pH 7.5). Each immunoprecipitation was repeated three times and figures show representative western blots.

2.7 Recombinant Protein Purification

Full-length mUCP3 was cloned into the pGEX-6P-1 vector with GST tag (GE Healthcare, Piscataway, NJ). Mouse DCI without the MTS was cloned into the pET-21b vector with 6XHis tag (mDCIΔMTS-6XHis) (Novagen, Madison, WI). Vectors were transformed into the competent BL21 (DE3) pLysS E. Coli strain and placed into a 37°C shaking incubator at 220 rpm. After reaching an OD of 0.3 (measured at 600nm), protein expression was induced by adding 1mM IPTG and returning the transformed bacteria to the shaking incubator for either 3 hours at 30°C (for pGEX-6P-1) or 3 hours at 37°C (for

pET-21b). The cells were then harvested by centrifugation at 8000xG for 10 minutes and stored at -80°C. Mouse UCP3 was diverted to inclusion bodies which required processing as previously described (Jaburek and Garlid 2003). Mouse UCP3 inclusion bodies were purified on a GSH column and DCI was present in the soluble fraction which was purified using a Nickel-NTA column (Qiagen, Valencia, CA).

2.8 GST Pulldowns

Purified glutathione S-transferase protein or GST-mUCP3 fusion protein (15µg) was prebound to glutathione-Sepharose 4 Fast Flow beads (GE Healthcare, Piscataway, NJ) in GST assay buffer (PBS with 600mM NaCl) then rotated for 16 hours at 4°C. After rotation, the beads were washed four times in GST assay buffer then incubated either alone or with 300ng mDCIΔMTS-6XHis. After incubation the beads were washed with GST assay buffer eight times and prepared for SDS PAGE. The pulldown assay was repeated three times and the figure shows a representative western blot and coomassie stained gel.

2.9 Isolation of Mouse Tissues

Mice were sacrificed via CO_2 asphyxiation and tissues were immediately harvested and placed in ice-cold CP-1 buffer (100mM KCL, 50mM Tris-HCl, 2mM EGTA, pH 7.4).

2.10 Isolation of Mitochondria

Tissues were finely minced in CP-1 buffer than transferred to a 30mL glass Potter-Elvehjem homogenizer. After 60 manual strokes, the homogenates were centrifuged at 500*g* then applied to a 40µm cell strainer to remove intact cells. The filtrates were then spun at 10,600*g* in microcentrifuge tubes to pellet the mitochondria. The pellets were resuspended in the appropriate lysis buffer for subsequent experiments.

2.11 Quantitative RT-PCR

Tissue or cells were harvested as described above and total RNA was isolated using TRIzol® reagent (Invitrogen, Carlsbad, CA). RNA was converted to cDNA per manufacturer's instructions using SuperScript II Reverse Transcriptase (Invitrogen, Carlsbad, CA). Sample cDNA was then amplified using iTaq SYBR Green Supermix with ROX (Bio-Rad Laboratories, Hercules, CA) and measured using a CFX96 Real-Time PCR Detection System (Bio-Rad Laboratories, Hercules, CA). Primers used were; mUCP3 sense 5'- ACTATGGATGCCTACAGAACC-3' antisense 5'-GACCCGATACATGAACGCT-3', mDCI sense 5'-CAGAGACTGCCCAAGGTCAT-3' antisense 5'-TGGCGTCCTTATCTTGGAAC-3', GAPDH sense 5'-AGAACATCATCCCTGCATCC-3' antisense 5'-GGTCCTCAGTGTAGCCCAAG-3'. Cycling conditions were initial denaturing 95 for 3 minutes, then 40 cycles of 95°C for 15 seconds and 55°C for 30 seconds. Analyses were repeated three times and data represent fold change relative to levels of GAPDH.

2.12 Mitochondrial Sublocalization Assay

We utilized the method of Whatcott et al. (Whatcott, Meyer-Ficca et al. 2009) with modifications. Briefly, mouse heart mitochondria were isolated as described above. Water soluble digitonin (MP Biomedical, Cleveland, OH) was used for permeabilization. After proteinase K treatment, the protease inhibitor PMSF was added at 2mM concentration to stop the reaction. Mitochondrial subcompartment marker antibodies used were as follows; anti-mitofusion, anti-aconitase (Abcam, Cambridge, MA) and anti-Cyt. C (Santa Cruz Biotechnology, Santa Cruz, CA). This assay was repeated three times and the figure shows a representative western blot.

2.13 Fluorescence Microscopy

For mitochondrial staining, the membrane potential sensitive dye TMRM was used. Live cells were stained with 25nM TMRM for 30 minutes at 37°C then washed three times with PBS. For nuclear staining, DAPI (Pierce Biotechnology, Rockford, IL) was used at a concentration of 50µg/mL. Equipment used for measuring mitochondrial, nuclear, and GFP fluorescence was; Nikon Eclipse Ti-S microscope, 60x Nikon Plan Apo VC Oil objective with numerical aperture 1.40, and a Photometrics Coolsnap EZ camera. Images were processed using Nikon NIS elements BR 3.0 Software. Each assay was repeated three times and figures show representative images.

2.14 Myocyte Oxygen Consumption

Skeletal muscle cell respiration rates were quantified using a Clark-type electrode (Insetech Laboratories, Plymouth Meeting, PA). Two million cells per sample were added to the 1mL chamber containing either HBSS (for glucose controls) or HBSS with 100µM water soluble oleic acid. The rate of oxygen consumption was obtained from linear regions of the slope observed with each treatment for three independent samples. Each assay was repeated three times and the figures shows mean oxygen consumption rates.

2.15 Primary Cell Isolation

We followed the method of Ojima et al. (Ojima, Uezumi et al. 2004). Skeletal muscle was removed from recently-sacrificed mice and minced in sterile, ice-cold PBS. The tissue was then digested in PBS with 10% FBS and 0.2% type II collagenase (Worthington Biochemical, Lakewood, NJ). After digestion, the tissues were filtered through 100µm and 40µm cell strainers. Samples were then spun at 800*g* for 5 minutes and the pellets were resuspended in hypotonic buffer (0.17M Tris-HCl Ph7.65: 0.83% NH_4Cl = 1:9 (V/V)). After 30 seconds, the suspended cells were diluted with 10mL PBS and spun at 800*g* for 5 minutes. The pellet was resuspended in growth media (HamF10 with 20% FBS) and applied to collagen coated plates then incubated at 37°C with 5% CO_2.

2.16 Bi-molecular Fluorescence Complementation

We used the Venus technology originally developed by Hu and colleagues (Shyu, Liu et al. 2006) which uses two vectors, each containing one half of the GFP protein. When the two halves come into close proximity, the GFP protein will be created and fluoresce. The Venus vectors pBiFC-VN173 and pBiFC-VC155 were obtained from the Addgene repository (Cambridge, MA). The N-terminal (amino acids 1-172) half of the GFP protein was subcloned into the pcDNA6mDCI-myc plasmid. The C-terminal (amino acids 155-238) of GFP were subcloned into the pcDNA3.1mUCP3-V5 (full length with C terminus in intermembrane space) and pcDNA3.1mUCP3ΔCt-V5 (with C terminus in mitochondrial matrix). The resulting fusion proteins were imaged by microscopy as previously described or on a Beckman-Coulter EPICS XL flow cytometer. Each assay was repeated three times and the figures show representative images.

2.17 Fatty Acid Oxidation

We employed the method of Mao et al. (Mao, Kraus et al.). H9C2 cells were grown in a 24-well plate then transiently transfected with the indicated plasmids. The transfected myotubes were placed in serum-free DMEM for 2 hours prior to changing to pre-incubation media (DMEM, 0.25mM oleate, 12mM glucose, 4mM glutamine, 25mM HEPES, 1% fatty acid free BSA) for one hour. Radiolabeled oleate or palmitate (American Radiolabeled Chemicals, St. Louis, MO) was added at a concentration of 1μCi/mL and the wells were immediately covered with filter paper. The cells were incubated for 1.5 hours at 37°C then the filter paper covering the wells was saturated with

3M NaOH and the cells were lysed with the addition of 70% perchloric acid. The radioactivity collected in the filter paper was measured via scintillation counting. Each sample was performed in triplicate and the assays were performed three times.

2.18 Animals

C57Bl6/J, B129, and FVB wild type mice were obtained from Jackson Laboratories (Bar Harbor, ME). C57Bl6/J UCP3 -/- mice were a gift of Dr. Marc Reitman, formerly of the National Institutes of Health. C57Bl6/J-hUCP3-α1actin-SKM-TG+/+ mice were a gift of Dr. Mary-Ellen Harper of the University of Ottawa. FVB-UCP1-DT mice were generated by Dr. Brad Lowell of Harvard University and obtained from Jackson Laboratories (Bar Harbor, ME). C57Bl6/J UCP1 -/- mice were a gift of Dr. Leslie Kozak of the Pennington Biomedical Research Institute. Animals were maintained on Prolab RMH 2000 5P06 chow and a 12 hour light/dark cycle. All procedures were approved by the University of Texas Institutional Animal Care and Use Committee (IACUC).

2.19 Intraperitoneal Temperature Probe Placement

The surgery was performed under sterile technique. Briefly, mice were given preoperative injections of 5mg/kg carprofen then the right dorsal flank was shaved and cleaned with sterile povidine solution. Isofluorane was administered via nose cone and after onset of general anesthesia a transverse oblique incision was made dorsally above the iliac crest. A similar incision was then made in the peritoneal wall and the wireless

temperature probe was inserted unanchored into the peritoneal cavity. The peritoneal wall incision was closed with nonabsorbable Vicryl sutures. The skin was closed with sterile skin staples. Animals were observed for signs of distress or infection for 72 hour prior to experiments.

2.20 Thermogenic Drug Administration

Male or female mice (~8 weeks of age) weighing between 20-25 grams were used for all studies. After a 48 hour recovery period, mice were moved to a temperature-controlled environment @ 25°C with *ad libitum* access to food and water. Mice were weighed and baseline temperatures recorded prior to subcutaneous administration of methamphetamine (25mg/kg), norepinephrine (1mg/kg) or lipopolysaccharide (25ng/kg) dissolved in vehicle (sterile water for injection). All doses were administered subcutaneously on the dorsal aspect of the animal sufficiently distant from surgical wounds.

2.21 Surgical Denervation of Intrascapular BAT

We used the method of Bartness & Wade (Bartness and Wade 1984) that was adapted from Foster and colleagues (Foster, Depocas et al. 1982) . Animals were prepared for surgery as described above. A transverse incision was made distally to the IBAT on the dorsal surface of the mouse in order to expose the subcutaneous fat layer. This layer of white fat was retracted to expose the two lobes of the IBAT pad. One incision was made on each lateral surface of IBAT pad in order to sever the 5 intracostal

nerves leading into the tissue. The skin was then closed with sterile skin staples. Animals were observed for signs of distress or infection for 72 hour prior to experiments.

2.22 Statistics

Statistical evaluation of qRT-PCR, western blotting, and FAO data was performed using the student's t-test with significance set *a priori* at $p<0.05$. Data represent averages with error bars representing standard error of the mean (SEM) from at least 3 independent experiments. For each experiment which assessed change in core body temperature, two groups were compared (experimental vs. control). A repeated measures analysis of variance (ANOVA) was performed to determine difference between the means of the two groups with significance set *a priori* at $p<0.05$. A *post-hoc* Student Newman-Keuls test was performed to assess pair-wise comparisons of individual timepoints from baseline. For the whole cell oxygen consumption experiment (Figure 3.9), we performed a 2-way ANOVA with significance set *a priori* at $p<0.05$.

Chapter 3 – Skeletal muscle UCP3 responds to diverse thermogenic stimuli

3.1 Introduction

UCP3 is expressed in skeletal muscle, brown adipose tissue (BAT) and heart (Boss, Samec et al. 1997; Gong, He et al. 1997). Among these tissues, UCP3-dependent mitochondrial uncoupling has only been observed in skeletal muscle, the most highly metabolic organ in humans – representing 40% of human body mass and 30% of overall oxygen consumption. Hyperthyroidism induces skeletal muscle UCP3 levels and temperature responses in humans and animals (Hesselink and Schrauwen 2005), but has little effect on BAT thermogenesis or UCP1 expression (Rothwell and Stock 1984; Petrovic, Cvijic et al. 2003). UCP3 in rodent BAT is thought to not mediate significant thermogenesis. BAT thermogenesis is normal in UCP3-deficient mice (i.e. they adapt normally to cold) (Nedergaard, Golozoubova et al. 2001), suggesting that UCP3-dependent heat production in response to amphetamines occurs outside of BAT. Previous studies have shown that the amphetamine compound MDMA significantly decreases skeletal muscle ATP levels *in situ, in vivo*, a marker of strong mitochondrial uncoupling (Rusyniak, Tandy et al. 2005). In most if not all cases, except in "Malignant Hyperthermia" (see Section 1.2.1. Hyperthermia and Heat Illnesses), thermogenic responses to physiologic stimuli (e.g. cold, feeding, infection, thyroid hormone) and pathologic stimuli (e.g. thyrotoxicosis, pheochromocytoma) are integrated centrally in the hypothalamus and lead to the activation of the sympathetic nervous system (SNS) and norepinephrine (NE) release into the bloodstream. NE primarily binds to β3-

adrenoreceptors in the endothelial, adipose, and skeletal muscle tissues (Chamberlain, Jennings et al. 1999). Upon activation, β_3-ARs mediate the liberation of free fatty acids (FFAs) and lead to their accumulation in the adipose tissue, bloodstream, and muscle. FAs in the bloodstream are taken up into thermogenic metabolically active tissues such as brown fat and skeletal muscle to be used as fuel for work or heat production. In cells, isolated mitochondria, and recombinant purified liposomal systems, FAs have been well established to be required for the activation of uncoupling proteins (Garlid, Jaburek et al. 1998). The pathway of activation for uncoupling proteins is listed in Figure 3.2. Thus, the goal of this investigation was to determine the anatomy of amphetamine-induced, UCP3-dependent thermogenesis (Figure 3.1).

.

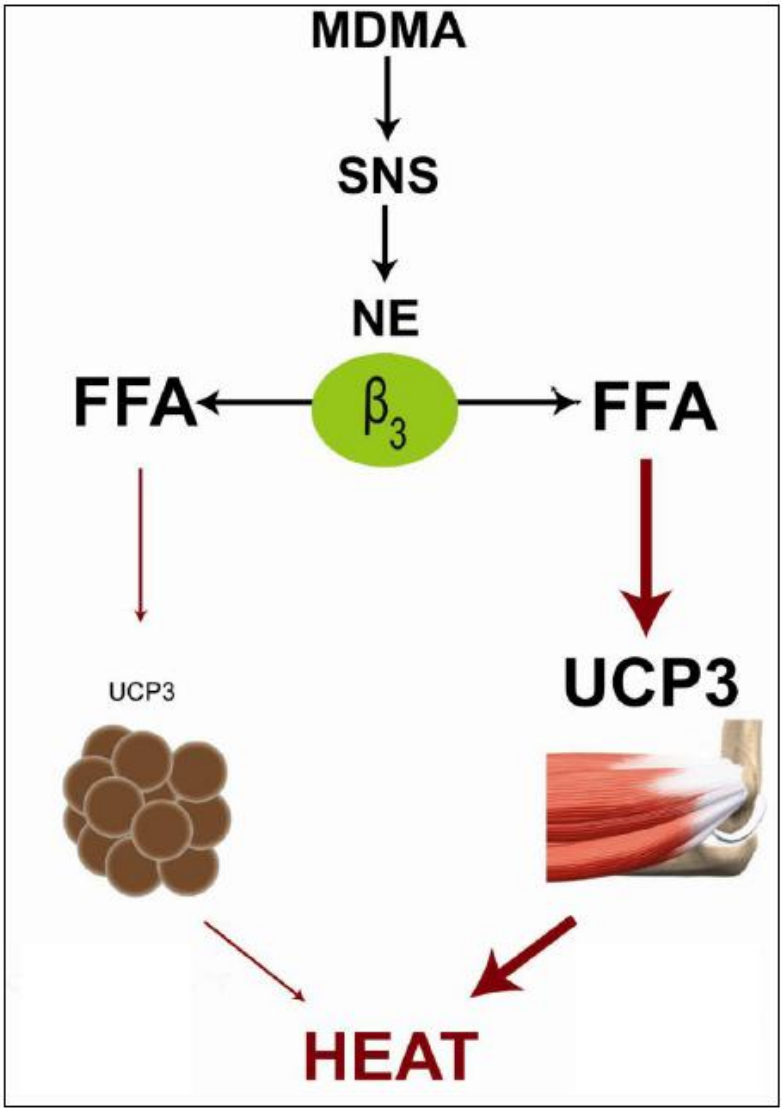

Figure 3.1 Two Potential Pathways For Amphetamine-Induced UCP3 Activation. UCP3 is expressed in brown adipose tissue (BAT) and skeletal muscle. Perhaps unlike muscle, BAT contains both the substrates (FAs) and targets (UCPs) within the same cell and tissue. In contrast a novel model is proposed whereby FAs originate in the more distant white adipose tissue (WAT) and travel through the vasculature to activate skeletal muscle UCP3.

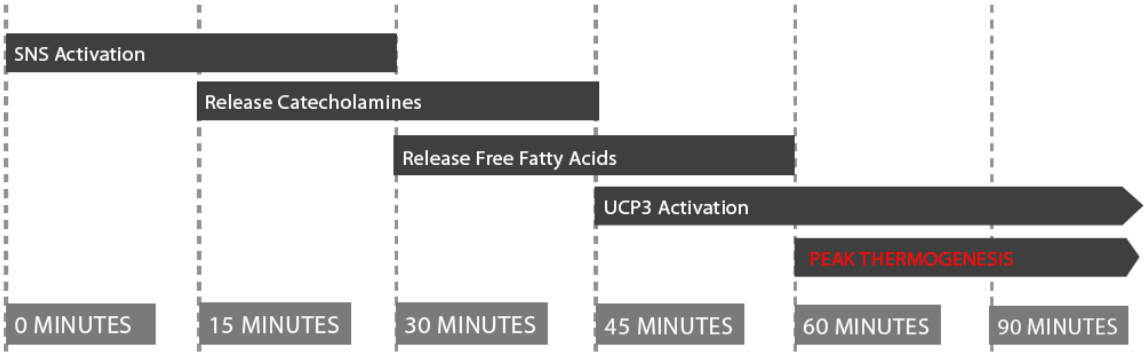

Figure 3.2 Timeline of Amphetamine-Induced Thermogenesis. Administration of amphetamines (e.g. methamphetamine, MDMA) causes activation of the sympathetic nervous system and release of catecholamines (e.g. norepinephrine, epinephrine, dopamine). Catecholamines bind to their β3-adrenoreceptors on adipose tissue to cause liberation of free fatty acids (FFAs). FFAs are taken up by skeletal muscle and cause UCP3 activation and thermogenesis. The pathway shown above represents the timeframe following subcutaneous amphetamine administration.

3.2 Results

3.2.1 Characterization of C57Bl6/J UCP3 -/- Knockout Mouse

The C57Bl6/J strain of mouse was used for the pivotal studies that established the UCP3-dependence for amphetamine-induced hyperthermia (Mills, Banks et al. 2003). However, the selection of this strain has received some criticism. Two main issues surround the use of these mice for temperature studies. **(1)** Wild-type C57Bl6/j mice are reported to have a large deletion in the gene encoding mitochondrial nicotinamide nucleotide transdehydrogenase (NNT), a transmembrane protein that transfers hydride ions between NADH and NADPH and their oxidized species (Freeman, Hugill et al. 2006). Therefore, theoretically, loss of *NNT* could lead to alterations in mitochondrial redox balance or proton motive force across the inner membrane that may augment UCP3 function (i.e. render UCP3 supraphysiologically thermogenic). Another possibility is that the loss of thermogenesis in the UCP3 null strain stems from a synthetic defect due to the combined deletion of both *NNT* and *UCP3* genes. We confirmed the deletion (exons 7 thru 11) of the *NNT* gene in our C57Bl6/j WT and UCP3 null mice, and that wild type *NNT* is present in B129 mice (Figure 3.3 A-B). **(2)** The loss of thermogenesis in UCP3-null mice could result from artifacts pertaining to the methodology used for UCP3 gene targeting and homologous recombination. For example, the C57Bl6/j UCP3 null strain was generated using B129 mouse stem cells that were used for the original gene targeting. B129 mice are purported to exhibit a thermoregulatory trait locus for ethanol hypothermia approximately 10.5 cM from the UCP3 gene located on 11q13.4 (Crabbe,

Belknap et al. 1994). Thus, a thermoregulatory mutation in the B129 strain could, albeit highly unlikely given the 10 backcrosses, mediate thermogenic defects unrelated to uncoupling protein 3 *per se*. Ruling out each of these possibilities, we show that B129 and C57Bl6/j mice have equivalent thermogenic responses to sympathomimetic drugs (methamphetamine, METH, Fig. 3.3 C), and have similar levels of skeletal muscle (SKM) mitochondrial UCP3 protein (Fig. 3.3 D). Figure 3.3 C shows that METH (20 mg / kg) induces overlapping body temperature responses in these different strains of mice. The experiment in Fig. 3C, and those in published work in rats, indicates that different rodent species and mouse strains respond to diverse sympathomimetic agents with highly similar thermogenic responses in terms of magnitude and time course changes in body temps. Thus, the UCP3 phenotype first established (Mills, Banks et al. 2003) is robust, and is independent of mouse strain and rodent species. Another important issue with regard to the phenotypes observed in the sympathomimetic-induced thermogenesis models deals with whether or not the effects are direct in terms of activation of UCP3, or are indirectly mediated by the activation of the sympathetic nervous system (SNS). The amphetamine MDMA has no direct uncoupling effects on muscle mitochondria (Rusyniak, Tandy et al. 2005), but rather appears to mediate its actions indirectly through activation of the SNS. In addition, the structurally distinct sympathomimetic amphetamine drugs 3,4-methylenedioxymethamphetamine and methamphetamine (MDMA, METH) induce similar patterns of thermogenesis in C57Bl6/j mice and UCP3-null mice are similarly protected from METH and MDMA hyperthermia (Sprague, Mallett et al. 2004).

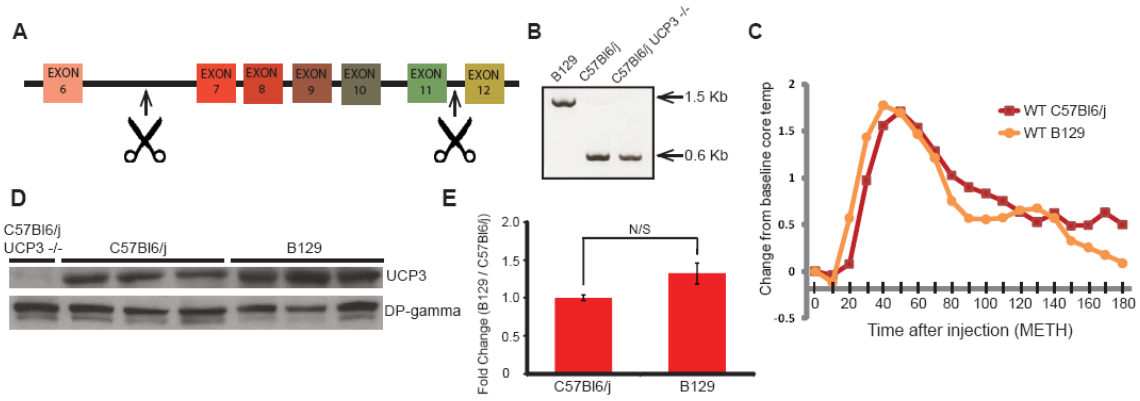

Figure 3.3 Loss of Sympathetic Hyperthermia in C57Bl6/J UCP3-/- Mice is Not a Strain Effect. *A*, C57Bl6/j mice have a large deletion mutation between exon 7 through exon 11 in the NNT gene indicated by arrows. *B*, RT-PCR (skeletal muscle mRNA) with primers to amplify from exon 6 thru 12 showing truncated NNT mRNA species in C57Bl6/j WT and UCP3 null mice, but a normal sized NNT mRNA fragment in B129 mice. *C*, B129 and C57Bl6/j mice (6-8 weeks) have identical sympathomimetic-induced (METH, methamphetamine, 20 mg/kg, s.c.) thermogenic responses (wireless temperature telemetry) over time (minutes). No significant difference was observed between groups (N=4) at any time point. *D*, Immunoblot shows similar amounts of UCP3 protein in isolated skeletal muscle mitochondria from B129 and C57Bl6/j mice. UCP3 -/- mitochondrial lysates are shown as an antibody control, and mitochondrial DNA polymerase gamma (DP-gamma) is shown as a loading control. *E*, densitometric analysis of the immunoblot in (d).

3.2.2 Generality of UCP3 in Thermogenic Responses

If UCP3 activation by MDMA and METH results from the sympathomimetic action of the drugs, then NE levels should increase prior to peak thermogenesis. Additionally, NE administration should elicit a decreased metabolic response in UCP3 knockout vs. WT mice. If UCP3 activation by METH / MDMA is physiologically relevant to thermoregulation in general, UCP3-null mice should exhibit a similarly diminished metabolic response to the bacterial pyrogen lipopolysaccharide. Recent data published in *Cell Metabolism* show that mice deficient in the prototypic UCP1 have only a modest, roughly 30% metabolic defect (oxygen consumption) in response to systemic administration of NE (1 mg/kg, sc) under normal dietary conditions (Feldmann, Golozoubova et al. 2009). Along with our preliminary and published observations, these data strongly support the notion that a significant, alternative thermogenic pathway exists that is UCP1-independent. We have published that levels of NE sharply increase (35-fold) in the bloodstream of rats 30 min. prior to peak MDMA-induced hyperthermia (60-90 min.) and that blockade of noradrenergic receptors (α_1 + β_3-adrenoceptor, AR) fully blocks hyperthermia induced by MDMA and METH (Sprague, Mallett et al. 2004; Sprague, Moze et al. 2005). As shown in Feldmann et al., 2009, in response to NE administration (1 mg / kg, sc), C57Bl6/j UCP3-null mice exhibit a large blunting (by roughly 70%) of peak (20 min.) of thermogenesis compared to WT (Fig. 3.4A). Using the bacterial pyrogen lipopolysaccharide (LPS), UCP3-null mice also show abrogated endotoxin-mediated fever (Fig. 3.4B). These experiments establish the physiologic

relevancy of both the sympathomimetic thermogenesis model and of UCP3 in thermoregulation in general.

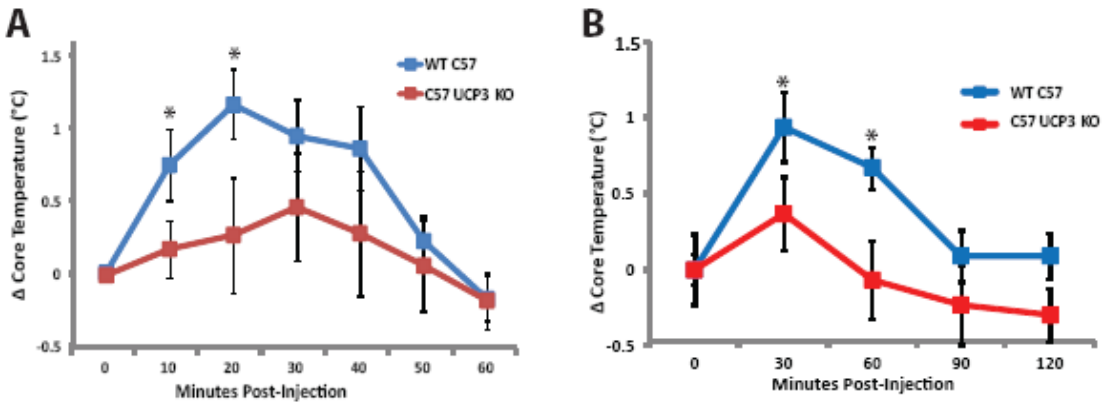

Figure 3.4. UCP3 knockout mice (C57Bl6/j UCP3 -/-) exhibit blunted thermogenesis to physiologic fever mediators. (a) WT and UCP3 KO mice (N = 4) were administered norepinephrine (NE, 1mg/kg, sc). WT mice exhibited a rapid and significant ($P < 0.05$, indicated by asterisks) peak increase over baseline in core body temperature at 20 minutes post injection. UCP3-null mice did not exhibit significantly increased body temperature from baseline at any time point. (b) WT and UCP3 -/- mice were administered the bacterial endotoxin lipopolysaccharide (LPS, 25ug/kg, sc). WT mice displayed a significant ($p < 0.05$, indicated by asterisks) febrile response over baseline, whereas UCP3 KO mice failed to generate a significant thermogenic response over the entire time course, and often develop significant hypothermia. A repeated measures analysis of variance (ANOVA) was performed to determine difference between the means of the two groups with significance set *a priori* at $p<0.05$. A *post-hoc* Student Newman-Keuls test was performed to assess pair-wise comparisons of individual timepoints from baseline.

3.2.3 Involvement of BAT in METH thermogenesis

Brown adipose tissue (BAT), although typically studied for its presence of UCP1 and strong contribution to cold-induced thermogenesis, also expresses UCP3. Thus, the UCP3-dependent phenotypes seen with certain genotypes cannot be assigned to solely one UCP3-expressing tissue. In this regard, the investigation into the tissue principally responsible for UCP3-dependent thermogenesis is crucial. Given the importance of BAT for cold-induced thermogenesis, it seems plausible that it is also responsible for responding to other types of thermogenic stimuli. If as hypothesized, the model (Figure 3.1) is correct that UCP3 in muscle is the anatomic site of sympathomimetic thermogenesis, then BAT ablation should have little or no effect on a UCP3-driven response. Figure 3.5 shows that METH induced heat production is modestly induced in mice bearing with partially (~70%) ablated BAT (FVB/N mice that express a UCP1 promoter diphtheria toxigene, FVB/N UCP1-DT) compared to wild type FVB/N controls (Figure 3.5). BAT ablated mice are also slightly more obese than wild type littermates (Figure 3.5). UCP3 is known to be upregulated in skeletal muscle in response to certain stimuli (e.g. fatty acids, PPAR agonists, fasting) (Boss, Samec et al. 1997; Boss, Samec et al. 1998). Skeletal muscles cells treated in vitro with both oleic and palmitic acids (C18:1, C16:0, respectively) show robust upregulation (Figure 3.6 Left). Conversely, brown adipocytes subjected to the same conditions show low basal expression levels and a lack of UCP3 upregulation in response to fatty acids. These data strongly support the model that skeletal muscle is a major site of UCP3-induced thermogenesis.

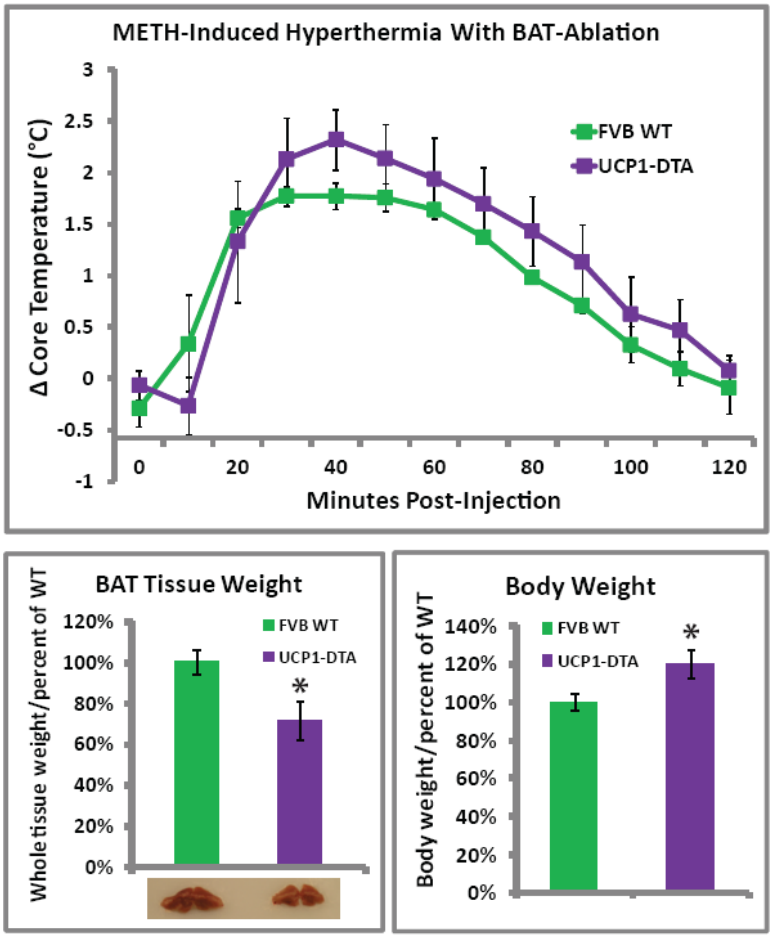

Figure 3.5 Ablation of BAT Does Not Affect Amphetamine-Induced Hyperthermia. Transgenic UCP1-DTA mice (N = 4) with partial (50-80%) ablation of brown fat induced by a UCP1-promoter-diphtheria toxigene have increased METH-induced (20 mg/kg, sc) peak thermogenesis, 30% reduction in total BAT tissue, and 20% increased body weight compared to WT mice. For the assessment of change in core body temperature (top graph), a repeated measures analysis of variance (ANOVA) was performed to determine difference between the means of the two groups with significance set *a priori* at $p<0.05$. No *post-hoc* test was performed because the difference between the two groups was not statistically significant. Statistical evaluation of BAT Tissue and Body Weight (lower panels) was performed using the student's t-test with significance set *a priori* at $p<0.05$. Data represent averages with error bars representing standard error of the mean (SEM) from at least 3 independent experiments. Shown below the bars in "BAT Tissue Weight" are typical intrascapular brown fat depots from WT and UCP1-DTA mice.

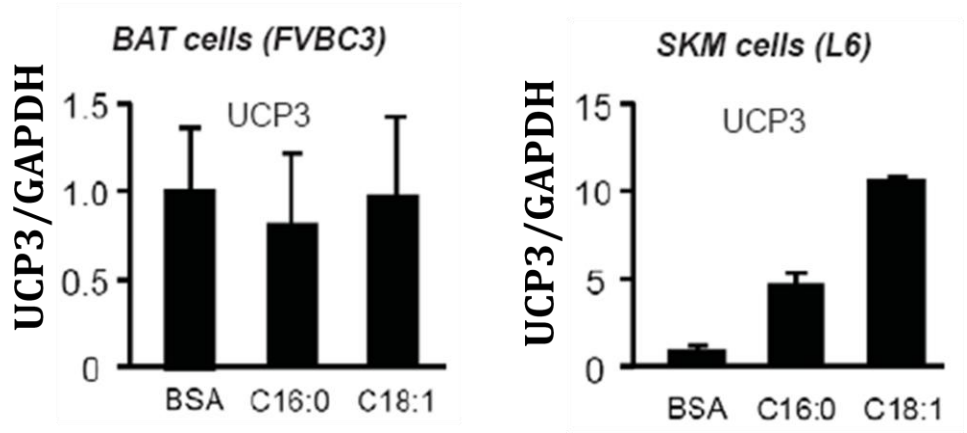

Figure 3.6 Levels of UCP3 in Skeletal Muscle, But Not BAT, are Responsive To Fatty Acid Treatment. *Left,* Levels of UCP3 mRNA (measured by qRT-PCR) are sharply induced in differentiated (5 days) C2C12 (mouse) and L6 (rat) myotubes in response to treatments with palmitic acid (C16:0) or oleic acid (C18:1) at 100uM for 24 hours. *Right,* UCP3 mRNA levels were unaffected by palmitic or oleic acid treatments in differentiated brown pre-adipocytes (FVBC3). Statistical evaluation was performed using the student's t-test with significance set *a priori* at $p<0.05$. Data represent averages with error bars representing standard error of the mean (SEM) from at least 3 independent experiments.

3.2.3 Skeletal muscle is a dominant site of FA-sensitive, UCP3-mediated thermogenesis.

Brown adipose tissue (BAT) and skeletal muscle (SKM) both express UCP3, and are the major metabolic and thermogenic tissues in animals. No evidence suggests that BAT UCP3 is thermogenic. As shown in Figure 3.5 above, partial ablation of brown adipose tissue has no effect on amphetamine-induced thermogenesis. In addition, in Figure 3.6 above, UCP3 is significantly upregulated in response to fatty acid treatment in skeletal muscle, but not brown adipose cells. To further scrutinize the thermogenic capacity of skeletal muscle UCP3, we used mice recently generated by Mary Ellen Harper's group that modestly (3-5 fold) overexpress UCP3 specifically but at physiological levels in skeletal muscle (hemizygous, alpha-1 actin promoter). Using these mice, we found that a non-thermogenic dose of METH in wild type C57Bl6/j mice induces a thermogenic response over baseline core body temperature in SKM-UCP3 overexpressing transgenic mice (Figure 3.7). The mice used in this experiment, do however, have intact endogenous UCP3 expression (including in BAT). In order to determine the thermogenic capacity of skeletal muscle UCP3 specifically, these mice were crossed with a UCP3 global knockout mouse. The resulting strain did not express endogenous UCP3 in any tissue, but did possess the skeletal muscle specific UCP3 expression at physiologic levels. In response to methamphetamine administration, these UCP3-/- SKM-UCP3 mice showed a hyperthermic response that was significantly higher than knockout littermates (Figure 3.8). This result confirms that UCP3 in muscle at

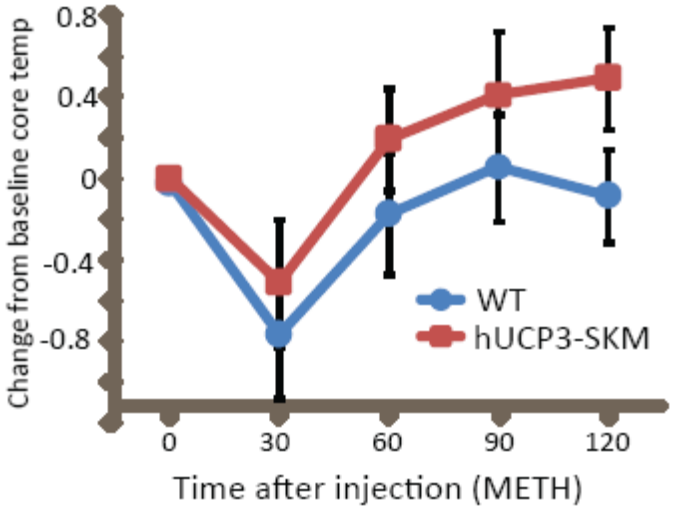

Figure 3.7 Skeletal Muscle Specific UCP3 Overexpression Augments Thermogenic Response to Amphetamines. Transgenic mice (N = 4) overexpressing UCP3 specifically in muscle (3-5 fold overexpression) show a detectable rise in body temperature over baseline to a non-thermogenic dose of METH (5mg/kg s.c.) that fails to induce thermogenesis in WT mice. A repeated measures analysis of variance (ANOVA) was performed to determine difference between the means of the two groups with significance set *a priori* at $p<0.05$. No *post-hoc* test was performed because the difference between the two groups was not statistically significant.

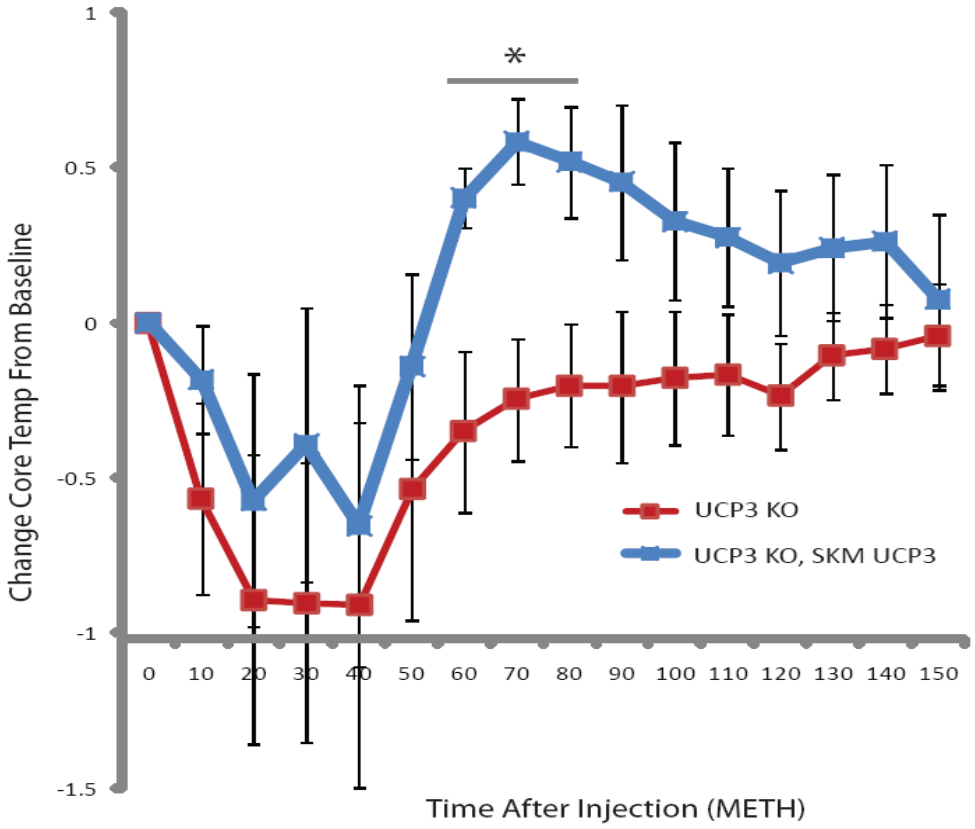

Figure 3.8 Absence of BAT UCP3 Does Not Prevent Amphetamine-Induced Thermogenesis. Transgenic mice overexpressing UCP3 specifically in muscle (3-5 fold overexpression) were crossed with UCP3 global knockout mice (N = 4). The presence of UCP3 in skeletal muscle only rescues the loss of effect METH (20 mg/kg, sc) seen in UCP3 knockout animals. * indicates significantly different from WT ($p < 0.05$). A repeated measures analysis of variance (ANOVA) was performed to determine difference between the means of the two groups with significance set *a priori* at $p<0.05$. A *post-hoc* Student Newman-Keuls test was performed to assess pair-wise comparisons of individual timepoints from baseline.

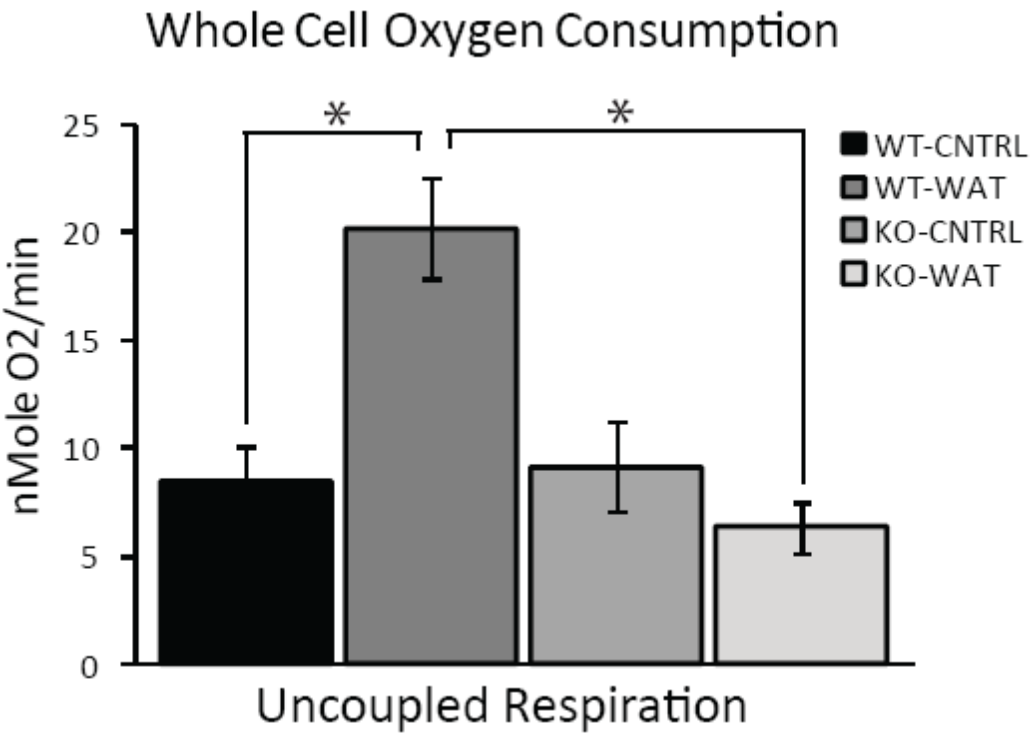

Figure 3.9 FFA Released From WAT Activate Skeletal Muscle UCP3. Differentiated white adipocytes were treated with either vehicle (CNTRL) or isoproterenol to stimulate lipolysis (WAT). The conditioned media was then applied to wild-type (WT) or UCP3 knockout (KO) skeletal muscle cells and thermogenesis was measured by indirect calorimetry using a respiration chamber fitted with a Clarke-type electrode (Instech labs). WAT but not CNTRL treated wild-type cells showed increased UCP3-dependent respiration. UCP3 knockout cells did not show a change after the addition of WAT versus CNTRL conditioned media. A 2-way ANOVA with significance set *a priori* at $p<0.05$ was used to compare WT-CNTRL to WT-WAT and then WT-WAT to KO-WAT. * indicates significantly different from WT ($p < 0.05$).

physiological concentrations is a thermogenic mediator. Consistent with a role for fatty acids in the response specifically in muscle, we isolated primary myoblasts from wild type and UCP3-null mice and differentiated cells for 5 days in low serum conditions (which induces UCP3 in WT cells, Figure 4.5 Left). Oleic acid-induced thermogenesis is significantly decreased in UCP3 knockout cells compared to WT (Figure 4.13 B). Although the direct application of fatty acids to skeletal muscle cells was able to activate UCP3, we also sought to determine if fatty acids released from white adipose tissue had a similar effect. We differentiated white adipocytes *in vitro*, then treated with either isopreterenol (3μM) or vehicle to stimulate lipolysis. The free fatty acid-containing conditioned media was harvested and used for skeletal muscle cell oxymetry (Figure 3.9). The WAT-conditioned media was able to induce uncoupled thermogenesis (as measured by indirect calorimetry) in skeletal muscle cells similar to treatment with fatty acids directly. UCP3 was required for this activation, as UCP3 knockout cells did not have an uncoupled respiration response to the WAT-conditioned media.

3.3 Conclusions

Brown fat (BAT) uncoupling protein 1 (UCP1) is the only established mediator of sympathetic nervous system-mediated heat generation in mammals. However, the low abundance of BAT and UCP1 in adult humans raises questions about its metabolic significance and clinical potential. The canonical view of thermogenic physiology was

built largely on the cold-induced, BAT thermogenesis pathway in rodents. As depicted in Figure 3.10, in response to cold, hypothalamic SNS activation leads to the release of

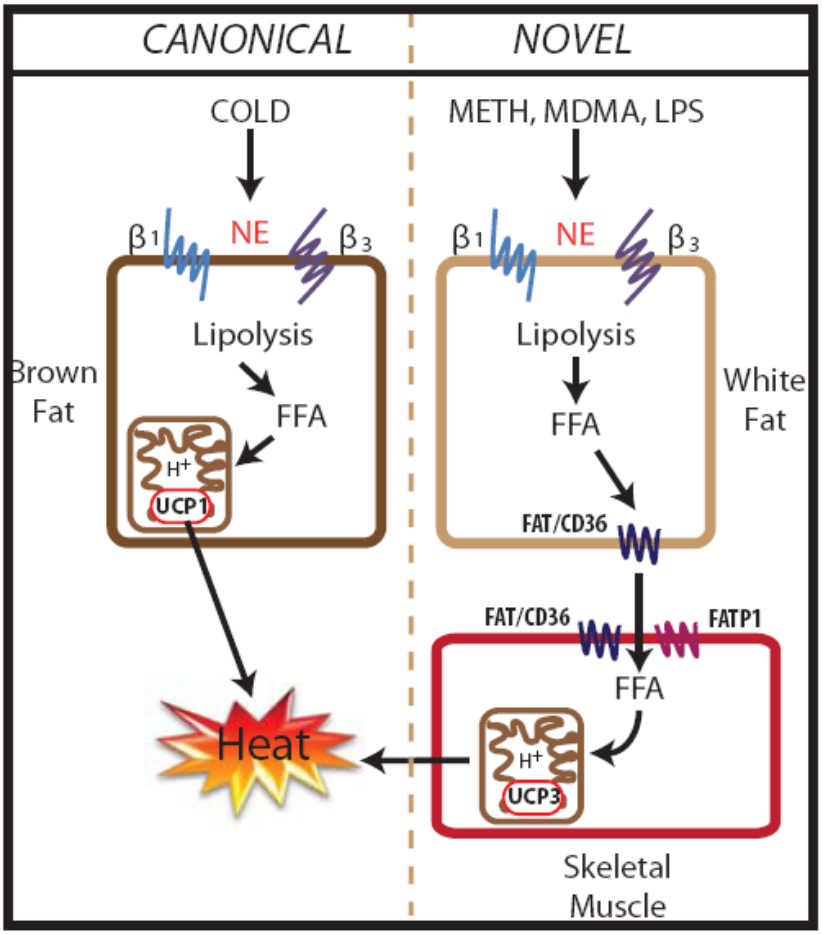

Figure 3.10 Canonical vs. novel UCP-dependent thermogenesis. The canonical pathway of UCP thermogenesis is based upon brown adipose tissue (BAT) which contains both the substrates (FAs) and targets (UCPs) within the same cell and tissue. In contrast a novel model is proposed whereby FAs originate in the more distant white adipose tissue (WAT) and travel through the vasculature to activate skeletal muscle UCP3.

norepinephrine (NE) from sympathetic nerves that richly innervate BAT. In turn, NE binds and activates plasma membrane beta adrenergic receptors (β-AR) on BAT adipocytes, leading to the activation of lipases that catalyze the liberation of fatty acids (FA) from triglycerides. FAs in turn are transported to mitochondria, where they bind UCP1 and activate thermogenesis. In this system, both the substrate for (FA) and the mediator of (UCP1) thermogenesis co-exist in the same cell (reviewed in (Nedergaard, Golozoubova et al. 2001)). We and others have observed that another SNS-induced thermogenesis pathway likely exists. First, UCP1 knockout mice lose only a small, albeit significant portion of the thermogenic response to NE administration compared to wild type (Feldmann, Golozoubova et al. 2009). UCP3 knockout mice exhibit a larger blunting of both sympathomimetic- (synthetic amphetamines) and norepinephrine-induced thermogenesis compared to their wild type littermates (Mills, Banks et al. 2003). Similarly, UCP3 is an important thermogenic target of thyroid hormone-induced body temperature regulation in muscle (Flandin, Donati et al. 2005; Sprague, Yang et al. 2007). Finally, it was recently demonstrated that systemic administration of sympathomimetic agents blunts brown fat thermogenesis (Rusyniak, Ootsuka et al. 2008). Based upon these observations and the data above, we propose that an alternative, novel pathway of thermogenesis exists wherein white adipose and skeletal muscle UCP3 participate in the thermogenic responses to sympathomimetic drugs (e.g., methamphetamine, METH) and the bacterial pyrogen lipopolysaccharide (LPS, Fig. 3.4 B). In this model, increased levels of circulating NE activate β-AR on white adipocytes, leading to the production of thermogenic FA and their release into the bloodstream (via the FAT/CD36 FA exporter

in white adipocyte plasma membranes). In turn, FAs are imported into skeletal muscle (via FAT/CD36 and FATP1 transporters), where they fuel UCP3-dependent thermogenesis. This proposed model is based upon the following observations; 1) Hormonal and genetic approaches to selectively increase UCP3 in skeletal muscle augemtn sympathomimetic-mediated thermogenesis. 2) Partial ablation (70%) of brown fat, a cold-activated thermogenic organ where UCP3 is also expressed, had no effect onsympathomimetic-mediated heat generation. 3) Fatty acid-induced thermogenesis (by indirect calorimetry) in muscle cells was significantly blunted in UCP3-null compared to wild type cells.

Chapter 4 – UCP3 Directly Binds $\Delta^{3,5},\Delta^{2,4}$ Dienoyl-CoA Isomerase to Augment Unsaturated Fatty Acid Oxidation

4.1 Introduction

Derangements in human energy balance involving an interaction between genes and environment contribute significantly to metabolic disease and likely underlie the recent epidemic of obesity, metabolic syndrome, and diabetes. At the cellular level, energy balance is regulated primarily though the oxidation of energy consumed in mitochondria, and the storage of energy not combusted as fat, protein, glycogen, etc. Mitochondrial respiration operates as a balance between substrate availability and energy requirements. Mitochondria generate energy by using a proton gradient to convert ADP and oxygen to ATP and water. Excess energy consumed relative to energy used (combusted, or spent) leads to obesity and its sequelae. The development of insulin resistance, particularly in skeletal muscle, has been reported as a major factor leading to the development of diabetes mellitus.

UCP3 regulates energy balance mechanisms in skeletal muscle and alteration of its function is linked in numerous clinical studies to obesity and diabetes in susceptible populations (Argyropoulos, Brown et al. 1998; Schrauwen, Xia et al. 1999; Schrauwen, Xia et al. 1999; Harper, Dent et al. 2002; Liu, Liu et al. 2005; Hsu, Niu et al. 2008). Mice lacking UCP3 exhibit increased oxidative stress and accumulation of fatty acids (Brand, Pamplona et al. 2002). Conversely, mice with a 2-5 fold increased UCP3 specifically in skeletal muscle are protected from diet-induced obesity and insulin

resistance (Choi, Fillmore et al. 2007). However, the mechanism behind this remains yet to be defined. Studies using genetic models of UCP3 overexpression have found an effect on metabolism of FAs and mitigation of ROS (Bezaire, Spriet et al. 2005). Several theories have been proposed to explain these effects. The most widely-held hypotheses for UCP3-dependent increased FAO are those originally proposed by Schrauwen (Schrauwen, Hoeks et al. 2006) and Harper (Himms-Hagen and Harper 2001), which support a model of extrusion of anionic fatty acids or lipid peroxides from the mitochondrial matrix.

$\Delta^{3,5},\Delta^{2,4}$ dienoyl-CoA isomerase (DCI) catalyzes the movement of protons along the fatty acid side chain to move double bonds in unsaturated fatty acids from odd to even positions to permit their normal beta oxidation to acetyl Co-A in both peroxisomes and mitochondria (Filppula, Yagi et al. 1998). Unsaturated fatty acids with odd numbered double bonds comprise an indispensable group of nutrients such as linoleic and linolenic, the essential fatty acids which are required for formation of arachidonate. Another DCI substrate, oleic acid is the principal fatty acid in olive oil, a major constituent of the human diet. Enoyl-CoA metabolites formed from these unsaturated FAs require auxiliary enzymes, such as DCI, in addition to the four primary beta oxidation enzymes (Luthria, Baykousheva et al. 1995; Shoukry and Schulz 1998; Gurvitz, Wabnegger et al. 1999). Accumulation of these metabolites poses a danger to the organism by exhausting stores of Co-A (Shoukry and Schulz 1998). Bacteria, which do not express DCI, must prevent accumulation of unmetabolizable enoyl-CoA species through export of the fatty acids into their growth medium. When permitted to accumulate in bacteria, these metabolites

inhibit normal beta oxidation (Ren, Aguirre et al. 2004). Likewise, knockout studies in C. Elegans have shown an increase in total fat content in the absence of DCI (Van Gilst, Hadjivassiliou et al. 2005).

Here we describe a novel protein-protein interaction between UCP3 and the auxiliary FAO enzyme DCI. In contrast to previous reports on UCP3 binding partners which have occurred outside the protein's terminal subcellular compartment (Pierrat, Ito et al. 2000), the UCP3-DCI complex exists in the mitochondrial matrix. DCI is present in each tissue that expresses UCP3 (skeletal muscle, heart, brown adipose tissue), and the UCP3-DCI complex forms at endogenous protein levels. The strength of binding was augmented with treatment with the DCI substrate oleate. Likewise, the UCP3-DCI complex increased oxidation of oleate. Mutational analysis of UCP3 and DCI revealed a consensus DxxK domain is necessary for binding and the effects on fatty acid oxidation.

4.2 Results

4.2.1 Interaction of UCP3 and DCI

Identifying binding partners for membrane integrated proteins can prove difficult because some domains may not be accessible when in its native, folded state. To combat this problem, the 7 hydrophilic domains of mouse UCP3 were used as probes (Figure 4.1). Hydrophilic domain 5 was excluded as reliable bait due to substantial false positive results. Using this strategy we probed a human heart library and identified the protein

$\Delta^{3,5},\Delta^{2,4}$ dienoyl-CoA isomerase (DCI) as a potential binding partner for hydrophilic domains 1, 3, and 4 of mUCP3 (Figure 4.2).

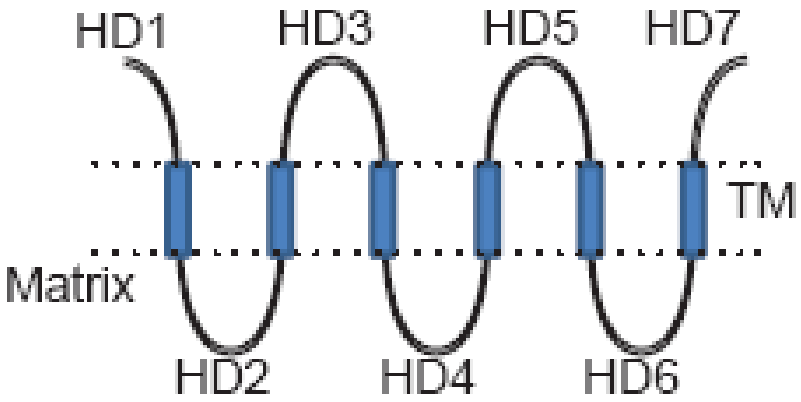

Figure 4.1 UCP3 Domain Structure. UCP3 structure: inner mitochondrial membrane localized UCP3 contains seven hydrophilic domains (HD1-7) connected by 6 transmembrane domains (TM).

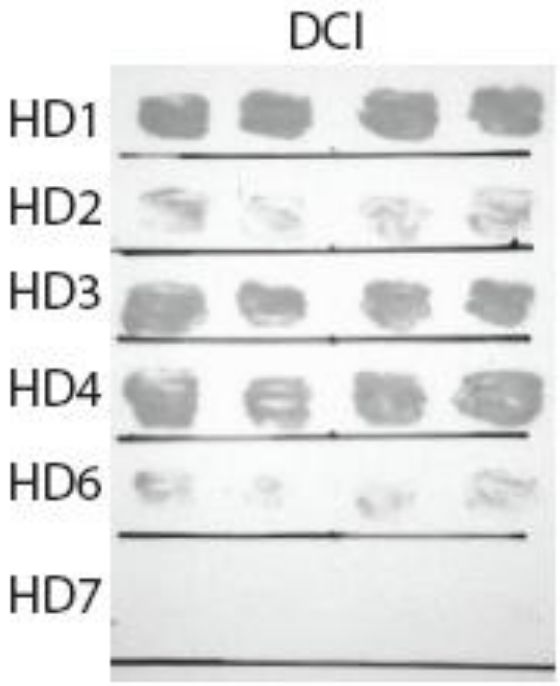

Figure 4.2 DCI Binds UCP3 Hydrophilic Loops Via Yeast-Two Hybrid. Growth phenotypes of yeast expressing full length DCI and individual UCP3 domains HD1-7 reveal that DCI may bind HD1, 3, and 4, but not HD2, 6, and 7.

DCI is an auxiliary fatty acid oxidation protein that exists in mitochondria and perixosomes, both of which are sites of beta oxidation in mammalian cells. The crystal structure of DCI has been studied and 4 primary domains have been identified. Studies performed in rat heart and liver mitochondria have shown the N-terminal ~43 amino acid mitochondrial targeting signal is not present within mitochondria and presumably cleaved upon import. The catalytic domain contains the two amino acid residues (E196, D204) shown to be necessary for retention of the protein's isomerase activity. DCI is thought to exist as a homotrimer with use of the trimerization domain that spans amino acids 249 to 313. The C-terminal end of DCI contains the 3 amino acid SKL sequence well-established as a non-cleavable peroxisomal targeting sequence (Figure 4.3).

In order to confirm expression patterns in a variety of tissues, the UCP3-containing tissues brown adipose, skeletal muscle, and heart were probed for both proteins (Figure 4.4). Liver was also used as negative control. DCI was found to have a similar expression pattern as UCP3. UCP3 is known to undergo significant upregulation in response to skeletal muscle differentiation. C2C12 mouse skeletal muscle cells were analyzed via quantitative real-time PCR and although UCP3 was upregulated levels of DCI were relatively unchanged (Figure 4.5).

Because the bait constructs used for the yeast two-hybrid analysis included hydrophilic domains present on both the matrix and intermembrane space sides of UCP3, we performed a mitochondrial sublocalization assay on DCI (Figure 4.6). Proteinase K treatment was used for protein digestion, along with increasing amounts of the membrane

permeabilizing detergent digitonin. With increasing detergent concentrations, the proteinase has more access to proteins previously protected by intact membranes. The mitochondrial outer membrane protein mitofusin was digested at a low digitonin concentration, whereas the intermembrane space protein Cytochrome C and matrix protein Aconitase were digested at much higher levels. DCI was digested at a similar concentration as Aconitase, indicating that it is also present in the mitochondrial matrix.

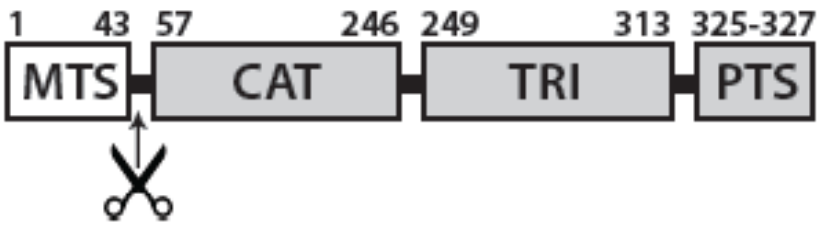

Figure 4.3 Structure of mDCI. DCI protein contains an N-terminal mitochondrial targeting sequence (MTS) followed by its catalytic domain (CAT), trimerization domain (TRI), and a putative peroxisomal targeting sequence (PTS).

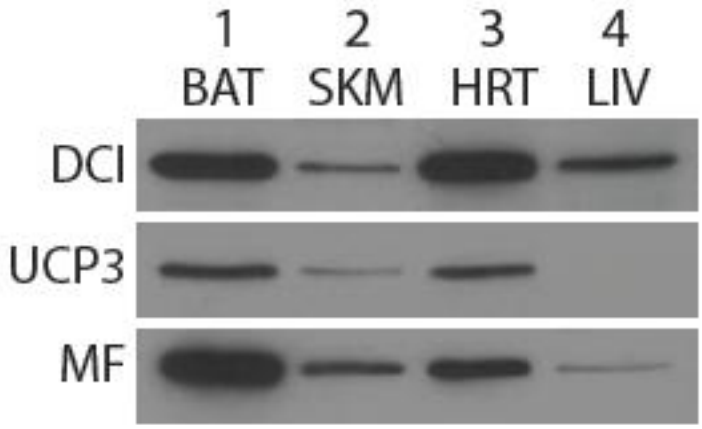

Figure 4.4 UCP3 and DCI Have An Overlapping Tissue Expression Pattern. UCP3 and DCI are co-expressed at similar levels in murine brown adipose tissue (BAT), skeletal muscle (SKM), and heart (HRT), but not liver. Immunoblot shows levels of DCI, UCP3, and the mitochondrial marker mitofusion (MF).

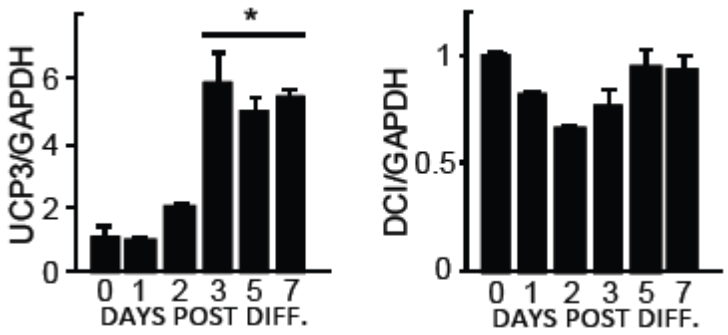

Figure 4.5 UCP3 and DCI Messenger RNA Expression In Muscle. Quantitative real time RT-PCR of UCP3 and DCI expression over a time course (days) of differentiation in C2C12 myotubes. Transcripts were normalized to GAPDH. Statistical evaluation was performed using the student's t-test with significance set *a priori* at $p<0.05$. Data represent averages with error bars representing standard error of the mean (SEM) from at least 3 independent experiments.

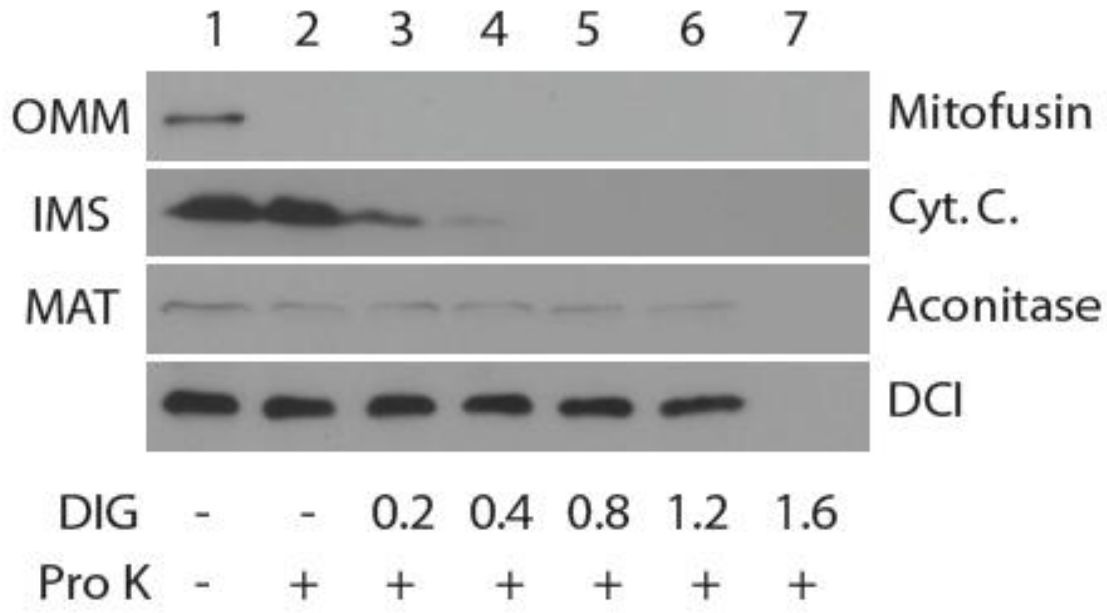

Figure 4.6 Mitochondrial sublocalization of DCI. Immunoblots show the presence of the outer mitochondrial membrane (OMM) protein mitofusin, the intermembrane space (IMS) resident cytochrome C (Cyt C), and the matrix (MAT) resident aconitase in mitochondria that were untreated or treated with proteinase K (Pro K) (lanes 2-7) and increasing concentrations of digitonin (DIG) (lanes 3-7, 0.2 to 1.6 mM DIG). OMM mitofusin immunoreactivity was lost with Pro K treatment, whereas IMS cytochrome C and matrix (MAT) resident aconitase required increasing digitonin concentrations for proteolysis. DCI was protected from the protease K / digitonin pretreatment to a similar degree as aconitase, indicating that it is localized to the mitochondrial matrix.

4.2.2 Expression and Localization of UCP3 and DCI

To check for accurate protein trafficking, the full-length DCI cDNA was cloned into a GFP-fusion vector and transiently transfected into HeLa cells (Figure 4.7). The membrane potential sensitive dye TMRM was used for detection of mitochondria for live cell imaging. DAPI stain was used to highlight the nuclear compartment. Upon overlay, the GFP fluorescence of the DCI fusion protein coincides with the red TMRM staining indicating that the transfected DCI protein traffics correctly to the mitochondria. In addition, cleavage of the mitochondrial targeting signal and mitochondrial localization was also confirmed via mass spectroscopy.

Next, we utilized HeLa cells to evaluate the interaction of DCI and UCP3 in mammalian cells (Figure 4.8). Full length mUCP3-V5 and mDCI-myc were transfected in equal amounts. Immuno-precipitation with antibody to myc tag revealed that mUCP3-V5 binds to mDCI-myc in this overexpression system. To control for another mitochondrial protein, the human adenine nucleotide transporter (hANT-myc) was used. Binding to mUCP3 was specific for mDCI and not hANT.

To test the binding of the endogenous UCP3 protein to mDCI, C2C12 mouse skeletal muscle cells were used (Figure 4.9). C2C12 cells exist as myoblasts until induced to differentiate into myotubes which begin to express UCP3 at Day 3. C2C12 cells were transfected with mDCI-myc and allowed to incubate for 48 hours prior to harvesting. Lysates prepared from Day 0 cells, as well as fully differentiated Day 7 cells were used for immunoprecipitation experiments. Antibody to myc tag or IgG control was used.

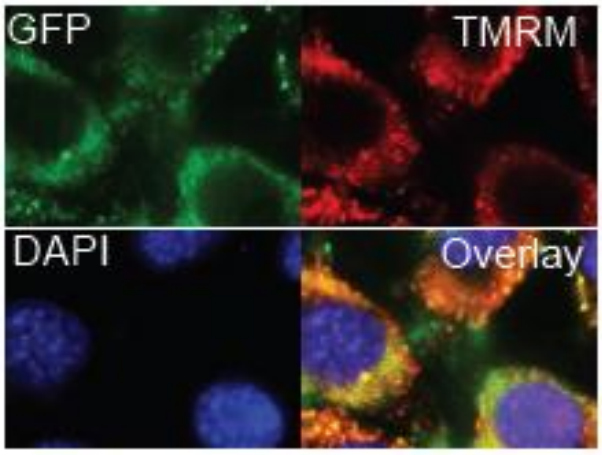

Figure 4.7 Fluorescence microscopy of DCI mitochondrial localization. DCI-GFP fusion protein is localized to mitochondria as indicated by overlapping staining with the mitochondrial indicator TMRM.

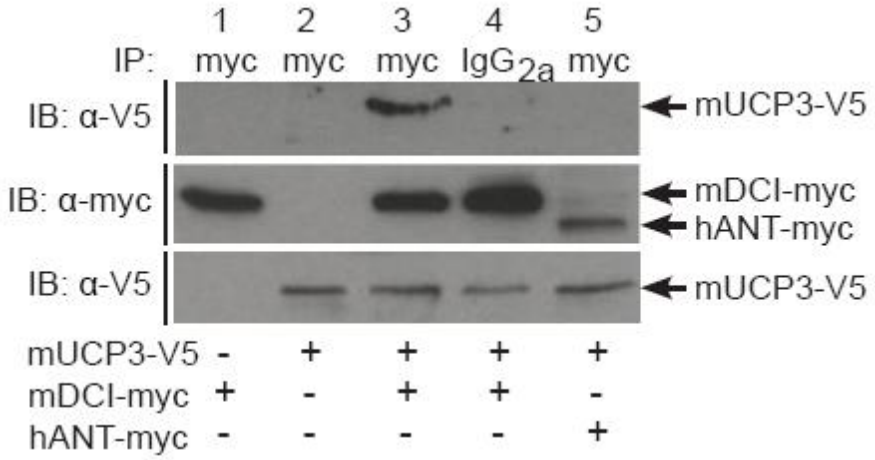

Figure 4.8 In Vitro Interaction of DCI and UCP3. Detection of the UCP3:DCI interaction in co-transfected HeLa cells. HeLa cells were transfected with the indicated plasmids mUCP3-V5, mDCI-myc, or hANT-myc (bottom). Lysates were immunoprecipitated (IP) with anti-myc antibody or the negative control IgG_{2A} and IP reactions were separated by SDS-PAGE and immunoblotted (IB) for anti-V5. UCP3-V5 (~36 Kd) was immunoprecipitated by the anti-myc antibody but not by IgG_{2A} in cells expressing mDCI-myc (lanes 3-4, upper panel). As a negative control, myc antibody failed to immunoprecipitate mUCP3-V5 from cells coexpressing hANT-myc and mUCP3-V5 (~36 Kd, lane 5, upper panel). Middle panel shows input for mDCI-myc (~37 Kd) and hANT-myc (~33 Kd). Lower panel shows input for mUCP3-V5 (~36 Kd).

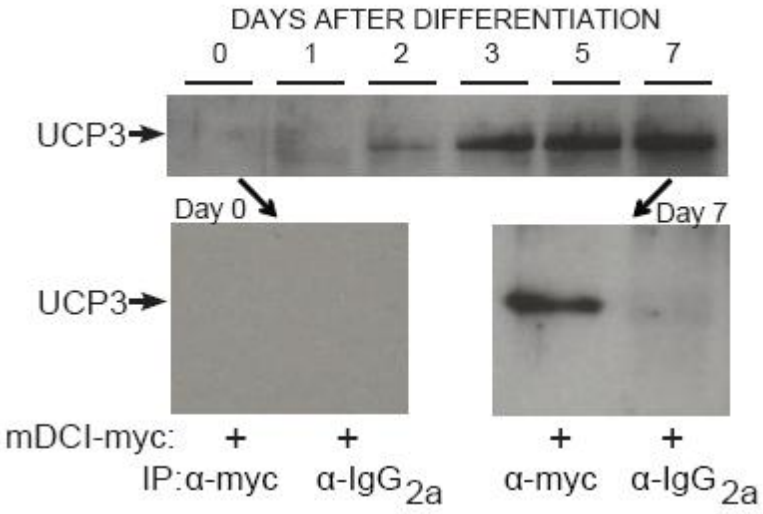

Figure 4.9 UCP3 and DCI Interact at Endogenous UCP3 Levels. C2C12 cells were differentiated for 1-7 days into mature myotubes then transfected with mDCI-myc. The upper panel shows endogenous UCP3 protein induction (~34 Kd) in isolated C2C12 mitochondria over time (days). (Lower panels) Lysates from day 0 (undifferentiated) and day 7 (differentiated) myocytes were immunoprecipitated with anti-myc or control IgG_{2A} antibodies. UCP3 immunoreactivity was immunoprecipitated by anti-myc only in the UCP3-expressing day 7 lysate and not by IgG_{2A}.

A

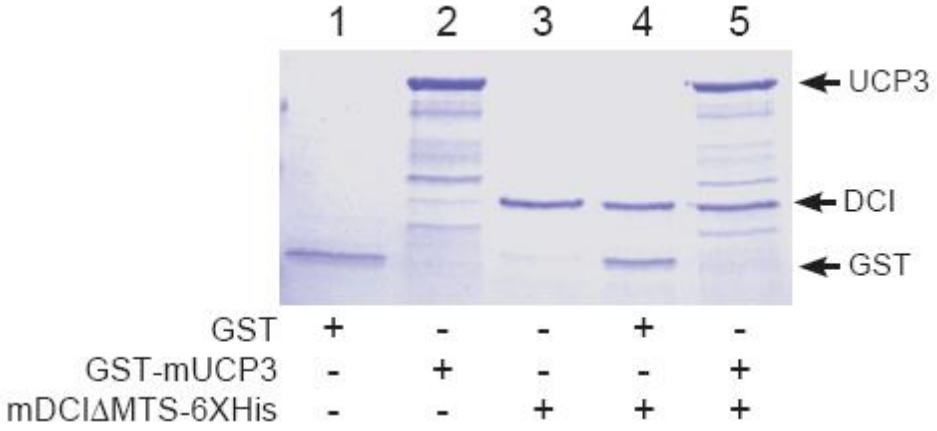

B

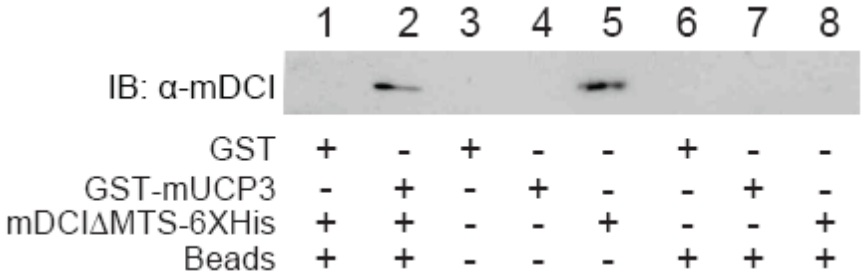

Figure 4.10 UCP3 and DCI Bind Directly *In Vitro*. *A,* Expression, isolation, and SDS-PAGE of purified recombinant GST-mUCP3 and mDCIΔMTS-6XHis from BL21 (DE3) E. Coli. Arrows indicate GST vector control (lane 1, ~26 Kd), GST-mUCP3 (Lanes 2, 5, ~60 Kd), and mDCIΔMTS-6XHis (lanes 3-5, ~35 Kd). *B,* Bacteria were transformed with the indicated constructs GST vector only (GST), GST-mUCP3, or mDCIΔMTS-6XHis and lysates were incubated with glutathione-coupled sepharose beads (beads). Pulldowns were subjected to SDS-PAGE and immunoblotted with a custom-made anti-DCI polyclonal antibody. As shown, DCI immunoreactivity (~35 Kd) was selectively pulled down by GST-mUCP3 (lane 2). Lane 5 shows the positive control lysates of cells expressing mDCIΔMTS-6XHis alone.

Only the Day 7 samples successfully immunoprecipitated endogenous UCP3 protein with anti myc tag antibody.

In order to determine if the UCP3 and DCI bind directly or require another protein or cofactor that is present in cells, a purified, recombinant interaction system was used. Full length mUCP3 was cloned into a pGEX6-P1 expression vector which creates a recombinant protein with an N-terminal GST tag. Because mDCI gets trafficked to the mitochondrial matrix, then undergoes cleavage of its targeting signal, it will not encounter UCP3 as a full length protein. Therefore, mDCI without its MTS was cloned into a pET21b expression vector to include a C-terminal 6X His tag. Full length UCP3 binds DCI in an *in vitro*, purified recombinant system indicating that direct binding can occur (Figure 4.10).

4.2.3 Mutational Mapping of the UCP3:DCI Binding Domain

To investigate the region of UCP3 responsible for DCI binding, we generated truncation mutants that lack each of the hydrophilic domains (except HD1). All constructs expressed as fusion proteins with the V5 tag and trafficked correctly to the mitochondria (data not shown). HeLa cells co-transfected with full-length DCI or UCP3 truncation mutants and then lysates were prepared and subjected to immunoprecipitation (Figure 4.11). While all truncation mutants bound DCI, the construct lacking matrix loop 2/hydrophilic domain 4 (HD4) exhibited altered binding characteristics. Notably a slight interaction remains in the HD4 UCP3 mutant, suggesting that the conserved DVVK-type domains in the first and third matrix loops, among other possibilities, may also participate

A

B

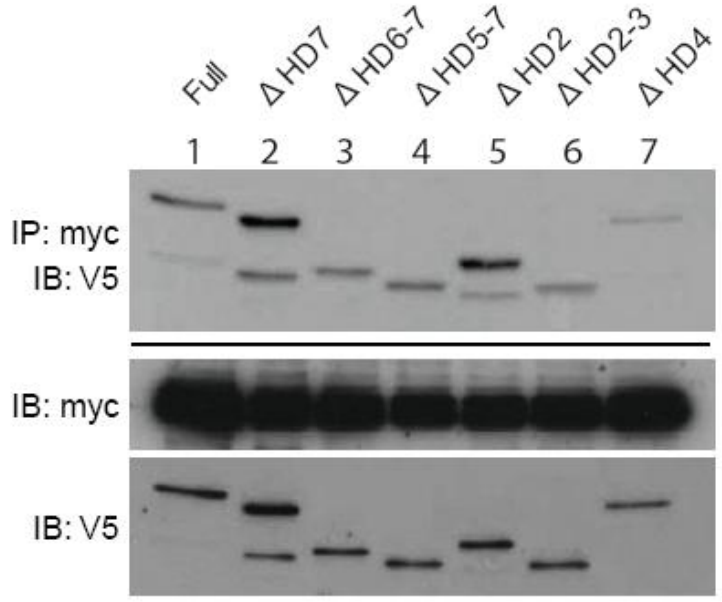

Figure 4.11 Binding of UCP3 HD truncation mutants to DCI in mammalian cells. *A,* Depiction of the mUCP3-V5 hydrophilic (HD) domain truncation mutant constructs used for DCI binding analyses. *B,* Cells were co-transfected with DCI-myc and the indicated V5 tagged full length UCP3 or UCP3HD mutants as indicated (top). Lysates were immunoprecipitated (IP) with anti-myc antibody and immunoblots (IB) were probed with anti-V5. The mutant lacking central matrix loop HD4 (ΔHD4, upper panel) showed strongly decreased binding to mDCI. Middle panel shows input for DCI-myc, and lower panel shows input for UCP3 and UCP3 HD mutants.

in DCI:UCP3 binding. To further scrutinize the residues important for binding, 3 additional mutants were made each lacking one third of the HD4 domain (Figure 4.12). After immunoprecipitation, the HD4A mutant, lacking the domain DVVK of UCP3 matrix loop 2 had an almost complete abolishment of binding (Figure 4.12). Sequence alignment revealed a similar motif contained within the trimerization domain of DCI at amino acid positions 134-146 (DIIK).

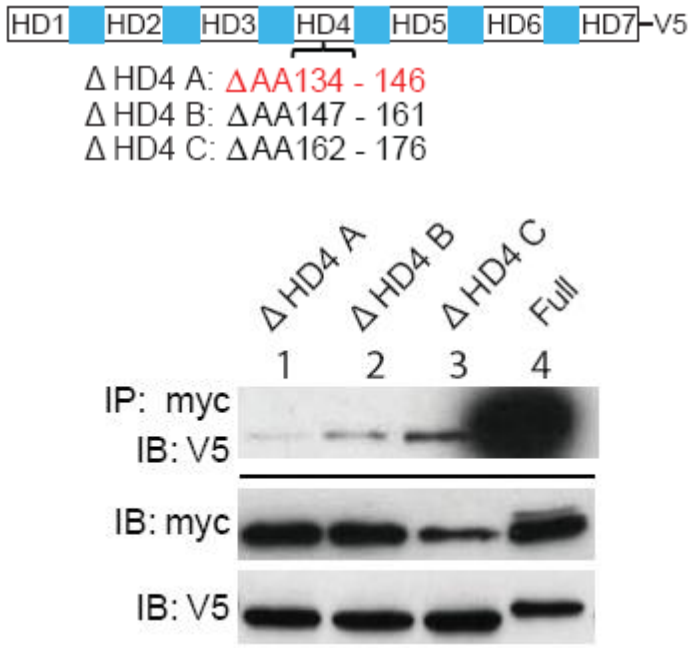

Figure 4.12 UCP3 and DCI interact via the first 12 amino acids of the central matrix UCP3 loop. The N-terminal (HD4A), middle (HD4B), and C-terminal (HD4C) thirds of UCP3 HD4 were truncated to further localize the UCP3:DCI interaction domain. Full length UCP3 or each UCP3 HD4A-C mutant was expressed in cells along with full length mDCI. Immunoprecipitations (as performed in B) show that the HD4A mutant poorly binds DCI (upper panel). Shown also are the inputs for DCI-myc (middle panel) and UCP3 HD4 mutants (lower panel).

4.2.4 Nutrient Sensitivity of the UCP3 – DCI Interaction

The activation of UCP3 by fatty acids, particularly unsaturated fatty acids has been well-established. The substrates for DCI, likewise, are unsaturated fatty acids, such as oleate. Consistent with these facts, we observed via qRT-PCR the significant upregulation of DCI and UCP3 in response to oleate treatment more so than the saturated FA palmitate (Figure 4.13 A). Using wild type and UCP3 knockout primary mouse myotubes, we discovered that oleate-induced thermogenesis (indirect calorimetry) is largely UCP3-dependent (Figure 4.13 B). Again using cells isolated from the skeletal muscle of WT or UCP3 KO mice, immunoprecipitation was performed after treatment with oleate and chemical crosslinking. When immunoprecipitated with anti-DCI antibody, a band is clearly visible in WT but not UCP3 KO lysates probed with anti-UCP3 antibody (Figure 4.14). This binding effect was exaggerated after a 16 hour treatment with 100μM oleic acid and was not due to substantial protein upregulation.

In order to test the binding effect in real-time, we utilized Venus bifluorescence complementation plasmids obtained via Addgene and submitted by Hu (Purdue University). These vectors each contain one half of the GFP protein which is expressed as a fusion protein. When these two halves (VC and VN) are expressed on other proteins which come into close contact, as during binding, they will form a full-length GFP protein which will fluoresce. Two mUCP3 constructs were cloned into the VC plasmid, one with the C-terminal tag in the inner membrane space (mUCP3-VC), and another with the tag in the mitochondrial matrix (mUCP3ΔCt-VC) (Figure 4.15). As predicted based upon the mitochondrial sublocalization of DCI, only the mUCP3ΔCt-VC construct

A

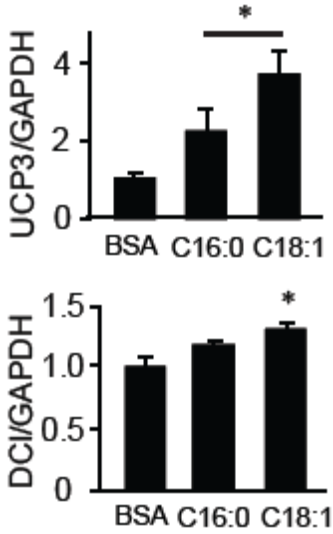

B

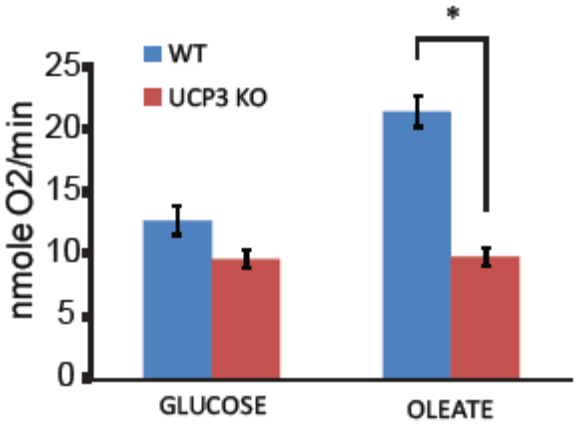

Figure 4.13 Sensitivity of DCI and UCP3 To Unsaturated Fatty Acids. *A*, Real time RT-PCR quantifications of UCP3 and DCI mRNA expression in C2C12 muscle cells after treatments with bovine serum albumin (BSA), oleate (C18:1) or palmitate (C16:0) normalized to GAPDH expression. *B*, Oleate-, but not glucose-induced thermogenesis (oxygen consumption / indirect calorimetry) is strongly blunted in UCP3 knockout (KO) compared to wild type (WT) primary differentiated murine myotubes. Statistical evaluation was performed using the student's t-test with significance set *a priori* at $p<0.05$. Data represent averages with error bars representing standard error of the mean (SEM) from at least 3 independent experiments.

produced fluorescence when co-expressed with mDCI-VN (Figure 4.15). To further explore the dependence upon fatty acids for binding, we co-transfected cells with mUCP3ΔCt-VC and mDCI-VN and subjected the cells to serum-free media or treatments of oleic acid (50µm, 100µM, or 300µM). Via microscopy, the dose-dependent increase in complementation fluorescence is clearly visible (Figure 4.16 A). Next, BSA and 300µM oleate treated samples were subjected to flow cytometry. A population of cells with increased fluorescence develops in the oleate treated samples (Figure 4.16 B).

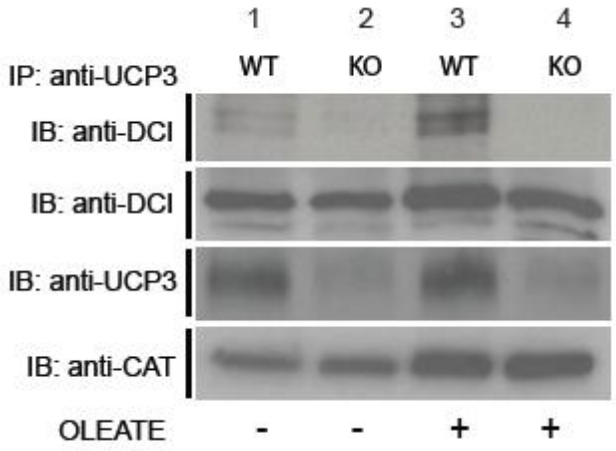

Figure 4.14 The UCP3 – DCI interaction in primary myotubes is oleate-sensitive. WT and UCP3 KO differentiated myotubes were treated with 300 µM oleate (16 hr) as indicated (below). Cell lysates were immunoprecipitated with anti-UCP3 followed by immunoblotting for anti-DCI. Upper panel shows that UCP3 specifically interacts with DCI in WT (lane 1, 3) but not UCP3 KO cells (lane 2, 4) in a manner strongly enhanced by oleate treatment (lane 3 versus lane 1). Input controls include immunoblots for anti-DCI, anti UCP3, and the loading control anti-catalase (CAT).

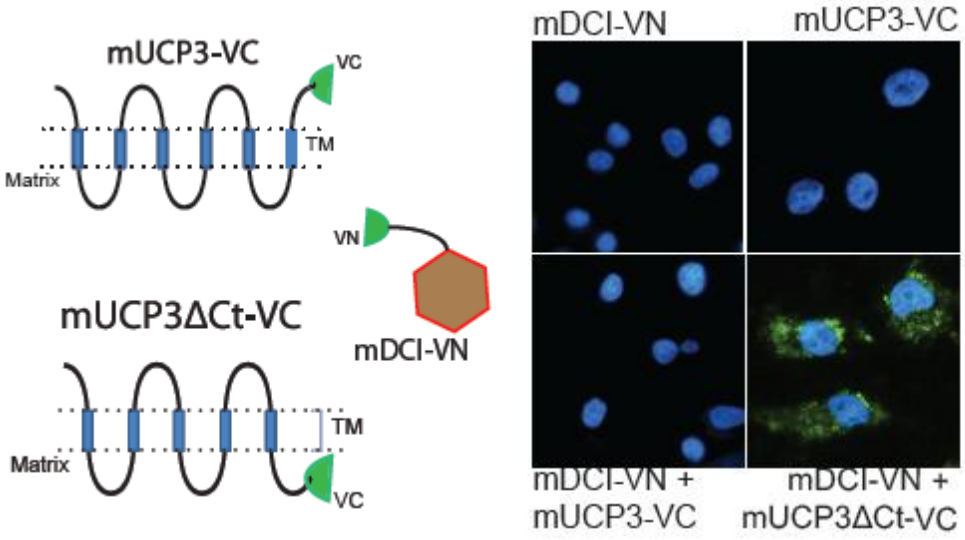

Figure 4.15 The UCP3 – DCI complex is formed specifically in the mitochondrial matrix in live cells. Hela cells were transfected with the indicated bimolecular fluorescence complementation probes containing N (VN) and C (VC) terminal tag split Venus GFP fluorophore fusion proteins with full length UCP3 (mUCP3-VC), a UCP3 truncation mutant that localizes the tag into the matrix (mUCP3ΔCt-VC), or full length DCI (DCI-VN). Cells were nuclear counterstained with DAPI. As shown in the lower right panel, only cells expressing mUCP3ΔCt-VC and mDCI-VN exhibited fluorescence complementation (note the punctate, perinuclear, mitochondrial pattern).

A

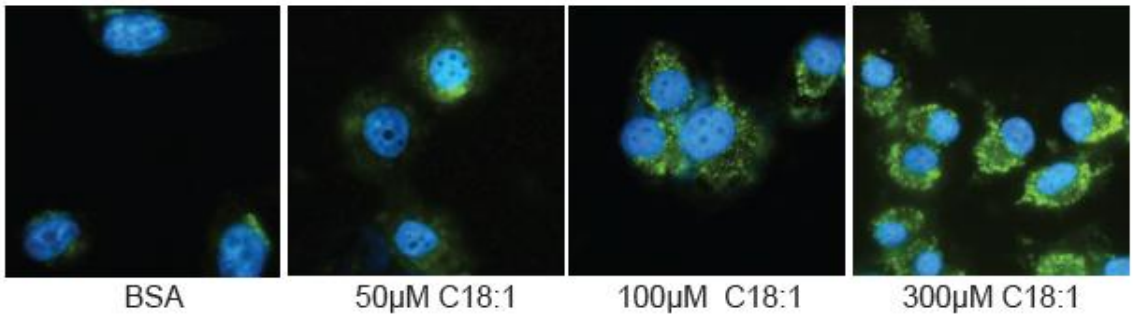

B

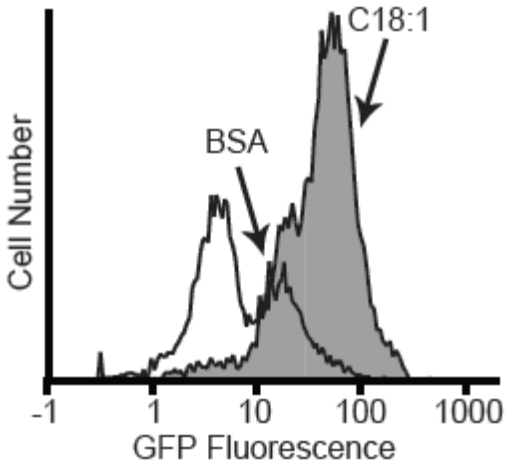

Figure 4.16 The UCP3:DCI interaction is increased by oleic acid in live cells. *A*, Cells cotransfected with mDCI-VN and mUCP3ΔCt-VC show increased mitochondrial GFP fluorescence complementation upon treatment with the indicated doses of oleate compared to the negative control BSA. Shown in *A* are fluorescence micrographs. *B* shows flow cytometric evaluation of the distribution of fluorescence. Clearly visible is the right shift in fluorescence in cells treated with oleate compared to BSA.

4.2.5 Functional Impact of the DCI – UCP3 Complex on Fatty Acid Metabolism

Previous studies showed that expression of DCI had no effect on mitochondrial membrane potential when overexpressed alone and no additive effect when coexpressed with UCP3 (data not shown). To investigate the effect on DCI activity, we employed an assay developed by Dong and colleagues (Mao, Kikani et al. 2006) using radiolabeled oleic acid to measure fatty acid oxidation. We used H9C2 heart myocytes because heart cells have very few peroxisomes compared to skeletal muscle. Therfore, transfected mDCI would likely shuttle to the mitochondria when transfected. When mDCI was overexpressed, no increase in FAO was seen and although mUCP3 produced an 8% increase above controls, this difference was not statistically significant. When both mDCI and mUCP3 are overexpressed, there is a synergistic increase in FAO above vector-transfected controls (Figure 4.17 A). This increase is not observed when a saturated fatty acid such as palmitate is used as the sole substrate (Figure 4.17 B).

Finally, to determine if the DxxK motifs in either UCP3 or DCI have an effect on binding or FAO, we generated the deletion mutants mUCP3ΔHD4A and mDCIΔDIIK. Immunoprecipitation with IgG control, as well as each wild type protein showed that deletion of either the DxxK in UCP3 or DCI was sufficient to abolish binding (Figure 4.18). As anticipated, the augmentation of FAO when both UCP3 and DCI are overexpressed was completely abolished with the deletion of either DxxK motif (Figure 4.19). Surprisingly, overexpression of both DxxK mutants showed a decreased level of FAO below wild-type controls, indicating that these mutants may act as dominant negatives.

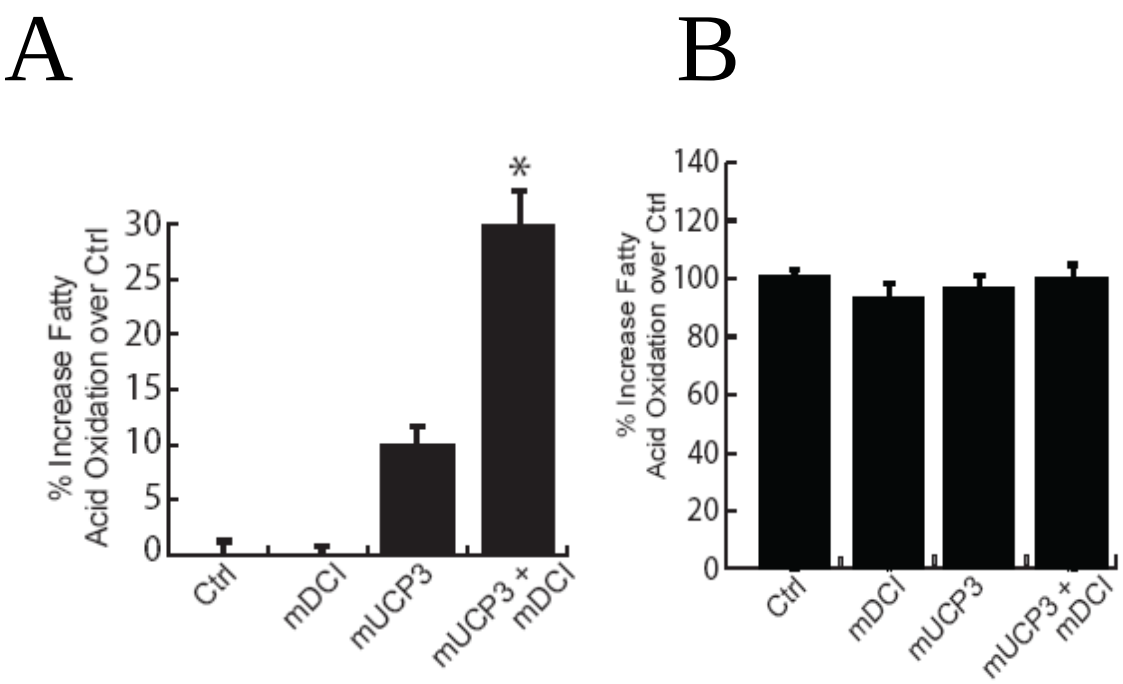

Figure 4.17 The UCP3 – DCI complex synergistically increases unsaturated fatty acid oxidation. ***A,*** H9C2 cardiomyocytes were transfected (efficiency ~ 50%) with the indicated plasmids and incubated with ^{14}C oleate. Accumulation of acid soluble $^{14}CO_2$ over time was used to monitor rates of fat oxidation and quantified by scintillation counting. Oleate metabolism was significantly increased only when both mUCP3 and mDCI were co-expressed. *B,* In contrast to unsaturated fatty acid oxidation, the UCP3 – DCI complex does not increase oxidation of the saturated FA palmitate. H9C2 cardiomyocytes were transfected (efficiency ~ 50%) with the indicated plasmids and incubated with ^{14}C palmitate. Accumulation of acid soluble $^{14}CO_2$ over time was used to monitor rates of fat oxidation and quantified by scintillation counting. Palmitate metabolism was unchanged with single transfection or when both mUCP3 and mDCI were co-expressed when compared to vector controls. Statistical evaluation was performed using the student's t-test with significance set *a priori* at $p<0.05$. Data represent averages with error bars representing standard error of the mean (SEM) from at least 3 independent experiments.

A

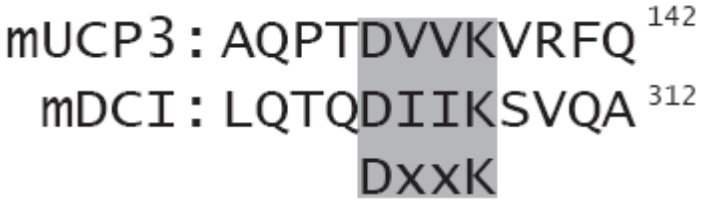

B

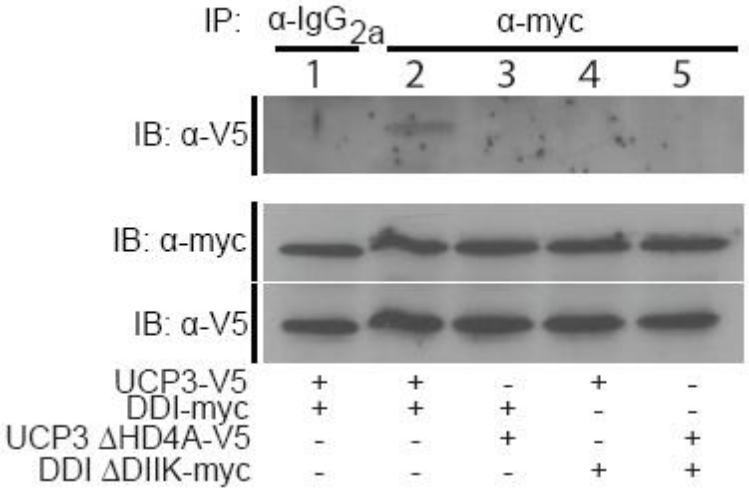

Figure 4.18 The DxxK Motif In UCP3 and DCI is Necessary For Binding. *A*, Sequence alignment reveals a homologous Asp X X Lys ($D_{xx}K$) putative binding motif in the 2nd matrix loop of mUCP3 and at amino acids 305-308 of mDCI. *B*, The DIIK motif in DCI confers binding to UCP3. HeLa cells were transfected with the indicated plasmids (below panels), immunoprecipitated with anti-myc or the negative control IgG_{2A}, followed by anti-V5 immunoblotting. As shown, only full length mDCI-myc bound full length mUCP3 (lane 2). UCP3-V5 was not bound by IgG_{2A} (lane 1), or by the mDCIΔDIIK-myc mutant (lane 4). As shown in Fig. 3, mDCI-myc failed to bind UCP3ΔHD4A-V5 which lacks the consensus $D_{XX}K$ motif (lane 3).

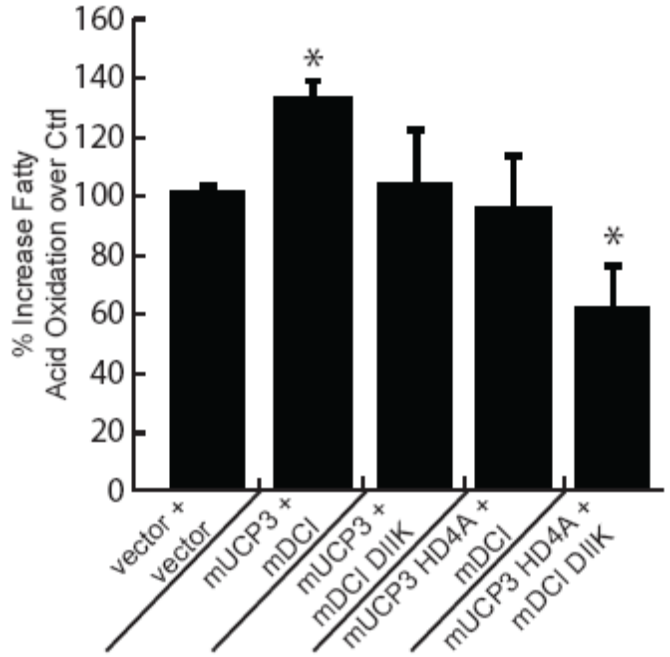

Figure 4.19 DCI – UCP3 binding is required for augmentation of oleate oxidation. H9C2 cardiomyocytes were transfected with the indicated plasmids and incubated with ^{14}C oleate. The augmentation of fatty acid oxidation seen with wild-type mUCP3 and mDCI overexpression was blocked by expression of either the mDCIΔDIIK-myc mutant or the UCP3ΔHD4A-V5 in combination with the wild type complex counterpart. Moreover, co-expression of mDCIΔDIIK-myc and UCP3ΔHD4A-V5 significantly decreased oleate oxidation compared to baseline vector only controls. Statistical evaluation was performed using the student's t-test with significance set *a priori* at $p<0.05$. Data represent averages with error bars representing standard error of the mean (SEM) from at least 3 independent experiments.

4.3 Conclusions

Experiments in cells, mitochondria, reconstituted liposomes, and planar lipid bilayers have demonstrated the requirement of FA for activation of UCPs (Jezek 1999; Skulachev 1999; Hagen and Lowell 2000; Zackova, Skobisova et al. 2003). However, little is known about the mechanisms by which fatty acids regulate UCP function. The bulk of literature indicates that UCP3 may function to coordinate the mitochondrial disposal (metabolism and transport) of fatty acids as a means of defending skeletal muscle from lipid and oxidant toxicity during conditions of increased fat oxidation (e.g. fasting, exercise, high fat diet)(Dulloo, Samec et al. 2001; Schrauwen, Hesselink et al. 2002; Schrauwen and Hesselink 2004; Brand and Esteves 2005). Indeed, UCP3 activation increases thermogenic fat oxidation and protects against obesity-induced insulin resistance and diabetes in mice (Choi, Fillmore et al. 2007). Saturated fatty acids (e.g. palmitate) are the prime culprits of metabolic suppression and inflammation induced by lipid overload (Weigert, Brodbeck et al. 2004). In contrast, recent work shows that both unsaturated fatty acids (e.g. oleate) and UCP3 increase lipid oxidation and protect from saturated fat-induced mitochondrial dysfunction and insulin resistance (Coll, Eyre et al. 2008; Gao, Griffiths et al. 2009). Coincidentally, unsaturated fatty acids (e.g. arachidonate, linoleate) are strong inducers of UCP-mediated proton leak *in vitro* (Zackova, Skobisova et al. 2003). We found that oleate sharply increases UCP3-dependent respiration in primary myotubes (Figure 4.13 B).

Interestingly, oleate and structurally-related “healthy” fatty acids require double bond isomerization prior to metabolism by beta oxidation (Ren and Schulz 2003). The

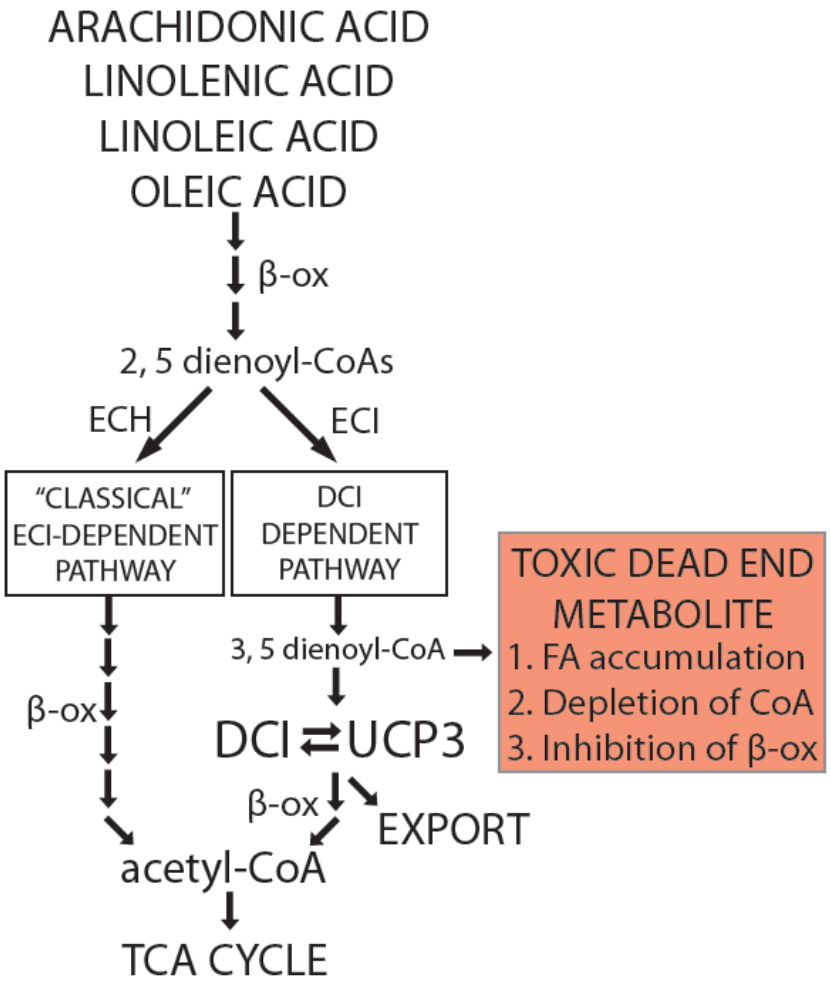

Figure 4.20 Proposed model of UCP3-DCI complex function. Unsaturated fatty acids, including arachidonate, oleate, and the essential FAs linolenate and linoleate, undergo hydrocarbon chain shortening by beta oxidation until the process is stalled by double bonds encountered at odd numbered carbon positions. Two pathways restore the beta oxidation of these metabolites. The 'isomerase-dependent' pathway does not utilize DCI. The 'DCI-dependent' pathway will produce FA species with double bonds in the 3 and 5 positions. DCI is the only enzyme identified that can metabolize these 3,5 dienoyl-CoA intermediates. Thus, without DCI, these intermediates would accumulate and sequester matrix CoA stores, leading to global inhibition of beta oxidation. UCP3, in addition to its protonophoric action, shares with DCI the proposed function of disposing of (through transport albeit) unmetabolizeable fatty acids. Thus, we propose a model where the UCP3:DCI complex functions as a fatty acid oxidation / proton transporting hub that matches unsaturated fatty acid metabolism with substrate and CoA availability and when necessary serves as a switch between oxidation and uncoupling.

auxiliary enzyme $\Delta^{3,5},\Delta^{2,4}$ dienoyl-CoA isomerase (DCI) is required for a percentage of metabolites produced by FAs with similar double bond configurations as oleate(Shoukry and Schulz 1998; Liang, Zhu et al. 1999). The ubiquitous tissue expression of DCI combined with its conservation through evolution in yeast, plant, and mammals suggest the importance of its function. We have shown, as in previous reports, that DCI contains a mitochondrial and peroxisomal targeting sequence (Filppula, Yagi et al. 1998; Zhang, Liang et al. 2001). The atypical presence of two targeting signals suggests DCI responds to nutrient sensing or selective shuttling to a certain subcellular compartment (mitochondria versus peroxisomes) as has been shown for other proteins (Elgersma, van Roermund et al. 1995; Lee, Lee et al. 2006).

We discovered that UCP3 interacts directly, at endogenous levels, and in an oleate-regulated manner with DCI (Figures 4.10, 4.14). Moreover, we also found that DCI:UCP3 synergized to increase oleic acid metabolism in myotubes (Figure 4.13 B). Finally, we observed that oleate treatment of primary myotubes increased the binding of UCP3:DCI in vivo, oleate-increased UCP3-dependent thermogenesis in wild type but not UCP3-null myotubes, (Figure 4.14) and C14 radiolabelled oleate metabolism was synergistically increased by the coexpressed wild type DCI and UCP3 compared to single DCI or UCP3 transfected myotubes (Figure 4.17 A).

Immunoprecipitation experiments with UCP3 mutants lacking amino acids 134-146, the first third of the central matrix loop, show strongly decreased DCI binding (Figures 4.11, 4.12). This same region contains an ASP Val Val Lys (DVVK) motif postulated by Jezek's group to be involved in fatty acid regulation of UCPs (Jezek and Urbankova

2000). Interestingly, a similar DIIK motif lies next to the active site pocket of DCI (Modis, Filppula et al. 1998) and thus may represent a common fatty acid interaction domain.

Combined, these results support our overall hypothesis that UCP3 mediates unsaturated FA-induced thermogenic lipid disposal. These findings are consistent with previous theories by Harper (Himms-Hagen and Harper 2001; Seifert, Bezaire et al. 2008) which propose UCP3 functions to maintain Coenzyme A availability, but not as an integral part of FAO. As represented in the proposed model (Figure 4.20), enoyl-CoA's produced from unsaturated FAs with double bonds in odd positions enter the beta oxidation system. Metabolites produced by enoyl-CoA isomerase (ECI) will shuttle FAs towards the 'reductase pathway'. Without the presence of DCI these metabolites would be allowed to accumulate, depleting CoA stores, and subsequently inhibiting beta oxidation. The UCP3:DCI complex serves to synergistically metabolize fatty acids through isomerazation of double-bonds and uncoupling.

Although previous knockout studies in yeast have shown little phenotype in the absence of DCI (Gurvitz, Mursula et al. 1999), other studies in C. Elegans have shown the robust and physiologically relevant consequence of FA accumulation (Van Gilst, Hadjivassiliou et al. 2005). Future directions for this research include the development of a DCI knockout mouse, which may have substantial morbidity depending on the percentage and type of fatty acids in the diet. In addition, determination of DCI: UCP3 complex activity and function from healthy and insulin-resistant diabetic skeletal muscle samples will be important. We predict that UCP3 and DCI interact in a nutrient-

dependent manner regulated by a consensus DxxK amino acid motif and when bound coordinately activate uncoupling and disposal of fatty acids, and protect from saturated fat-induced metabolic dysfunction.

Chapter 5 – Concluding remarks and future directions

Since its discovery in 1997, no consensus has been reached by the scientific community on its physiologic or biochemical functions of Uncoupling Protein 3 (UCP3). Thus, this work sought to address gaps in the knowledge surrounding UCP3 function through the study of its anatomical location of action and protein-protein binding partners. Although initially thought to play a role in cold-induced adaptive thermogenesis similar to UCP1, that theory was later disproven by the observation that UCP3 knockout animals respond normally to cold exposure (Vidal-Puig, Grujic et al. 2000). It is widely held that UCP1 is the only uncoupling protein able to mount an inducible thermogenic response in animals (Nedergaard, Matthias et al. 1999). Previous studies with MDMA (Mills, Banks et al. 2003) and our studies with methamphetamine, lipopolysaccharide showing that thermogenic responses to these agents are 80-100% attenuated in UCP3 knockout animals challenge this long held view. Our observation that skeletal muscle UCP3 can mediate a significant, non-shivering inducible thermogenic response therefore represents a significant paradigm shift.

UCP3 protein expression has been convincingly demonstrated in only three tissues – heart, brown fat, and skeletal muscle (Vidal-Puig, Solanes et al. 1997). Among these tissues, UCP3-dependent mitochondrial uncoupling has only been observed in skeletal muscle, the most highly metabolic organ in humans – representing 40% of human body mass and 30% of overall oxygen consumption. UCP3 in rodent brown adipose tissue is thought not to mediate significant thermogenesis; this is evident in large part because BAT (via UCP1) in UCP3 knockout animals generates heat and maintains

normal body temperature when animals are exposed to cold (Liebig, von Praun et al. 2004). A large misconception in the clinical and scientific literature concerning the mechanisms by which muscle generates heat is that it mainly involves some combination of shivering (muscle work / contraction), the sarcoplasmic Ca^{++}-ATPase ryanodine receptor, or other calcium handling mechanisms (McCoy, Renfrew et al. 1994). Shivering, which requires calcium for contraction, indeed is an early component of the thermogenic adaptation to cold and infection, and contraction or any manner of significant muscle work is thermogenic. However, shivering is not only metabolically demanding to the organism, but may also compromise oxygenation and is therefore disabling. Following cold exposure and infection, shivering apparently "kick starts" thermogenesis, but it soon wanes as non-shivering thermogenic responses take over. In response to feeding and activation of the SNS, shivering is not reported to play any role in the thermogenic response.

With regard to the ryanodine receptor, certain mutations in this protein in humans and pigs give rise to malignant hyperthermia, a rare pharmacogenetic disorder that expresses when patients are administered triggering agents such as volatile anesthetics. Dantrolene specifically binds and inhibits the ryanodine receptor, and is a very effective, life-saving treatment for malignant hyperthermia (Blank and Boggs 1993). However, despite its use in the clinic (because of the assumption that hyperthermia in people is *generally* ryanodine-dependent), no evidence establishes that dantrolene effectively lowers body temperature in response to any other hyperthermia or fever-inducing condition, including MDMA hyperthermia, septic fever, neuroleptic malignant syndrome,

thyrotoxicosis, etc. Likewise, it has been shown that dantrolene has no effect on MDMA-induced heat production in rats, indicating that the ryanodine receptor is not involved in the MDMA response (Rusyniak, Banks et al. 2004). Previously published studies show that ATP levels rapidly decline in skeletal muscle *in vivo* after MDMA administration, a hallmark of strong mitochondrial uncoupling (Rusyniak, Tandy et al. 2005). Since UCP3 mediates 80% of the thermogenic response to MDMA, all other potential mediators (UCP1, ryanodine receptor, etc.) play a relatively minor role (≤20% of the response). UCP3 in skeletal muscle may be a relevant mediator of human inducible thermogenesis.

In most, if not all cases, thermogenic responses to physiologic stimuli (e.g. cold, feeding, infection,) and pathologic stimuli (thyrotoxicosis, amphetamine hyperthermia, pheochromocytoma) are integrated centrally in the hypothalamus and lead to the activation of the SNS and NE release into the bloodstream. NE primarily binds to β_3-adrenoreceptors in endothelial, adipose, and skeletal muscle tissues. Upon activation B_3-ARs mediate the activation of lipases in target tissues leading to the systemic conversion of triglycerides (TGs) to free fatty acids (FFAs) and the accumulation of FA in the bloodstream, adipose, and muscle tissues. FAs in the bloodstream are taken up into thermogenic, metabolically active tissue such as brown fat and skeletal muscle to be used as fuel for work, or heat production. In cells, isolated mitochondria, and recombinant purified liposomal systems, FAs have been well established to be required for the activation of uncoupling proteins. Multiple fatty acid species and other lipid messengers bind and activate UCP-dependent proton leak across mitochondrial or liposomal

membranes (Matthias, Ohlson et al. 2000; Zackova, Skobisova et al. 2003). The highest affinity FA ligands for UCP1 and UCP3 include the long chain fatty acids oleic, palmitoleic, and lauric acids, and bind to each UCP with a similar affinity (Zackova, Skobisova et al. 2003). In addition, FA added to cultured primary brown adipocytes also directly activate UCP1 thermogenesis (Matthias, Ohlson et al. 2000). Thus, the activation of uncoupling proteins by fatty acids is likely intimately tied to their function.

The biochemical function of UCP3 has long been the source of speculation by many laboratories. It has been proposed to decrease reactive oxygen species (ROS), prevent insulin resistance, combat obesity, prevent lipotoxicity, and increase metabolism of fatty acids. In attempting to analyze UCP3 function by looking for protein bindings partners, we discovered a novel interaction with the fatty acid oxidation enzyme DCI. The complex formed by UCP3 and DCI is the first mitochondrial UCP3 protein interaction reported. In addition to its novelty, this complex also has functional consequences by increasing fatty acid oxidation and preventing accumulation of toxic lipid metabolites. The study presented herein provides supporting evidence for the inducible, thermogenic capacity of skeletal muscle UCP3. Likewise, through the discovery of protein binding partners, the role of UCP3 in preventing mitochondrial lipotoxicity is more clear. Collectively, the findings presented in this work will contribute to the understanding of thermogenic proton leak and energy wasting in humans.

In humans, the direct mechanisms that mediate thermogenesis in response to stimulation of the SNS have not been identified, and therefore no treatments exist for

most types of hyperthermic illness. Identification of thermogenic mediators is required for the development of anti-hyperthermic agents. On the other hand, safe stimulation of thermogenesis is a promising approach for the development of more effective anti-obesity therapies. This promising strategy also requires the identification of thermogenic mediators so that heat production can be more accurately titrated than is possible with current (and dangerous) thermogenic treatments (e.g. systemic stimulants, ephedra). We have identified a novel, UCP3-mediated thermogenic pathway that can be stimulated by a variety of inducing agent, in different animal species and mouse strains. These studies will offer new insights into thermoregulation in general. And are expected to illuminate molecular mechanisms by which uncoupling proteins may regulate proton leak and fatty acid metabolism that have remained largely unknown since UCP1 was first discovered some three decades ago.

References

Aiyagari, V. and M. N. Diringer (2007). "Fever control and its impact on outcomes: what is the evidence?" J Neurol Sci **261**(1-2): 39-46.

Andrews, M. T. (2007). "Advances in molecular biology of hibernation in mammals." Bioessays **29**(5): 431-40.

Argyropoulos, G., A. M. Brown, et al. (1998). "Effects of mutations in the human uncoupling protein 3 gene on the respiratory quotient and fat oxidation in severe obesity and type 2 diabetes." J Clin Invest **102**(7): 1345-51.

Azzu, V., M. Jastroch, et al. (2010). "The regulation and turnover of mitochondrial uncoupling proteins." Biochim Biophys Acta **1797**(6-7): 785-91.

Barreiro, E., C. Garcia-Martinez, et al. (2009). "UCP3 overexpression neutralizes oxidative stress rather than nitrosative stress in mouse myotubes." FEBS Lett **583**(2): 350-6.

Bartness, T. J. and G. N. Wade (1984). "Effects of interscapular brown adipose tissue denervation on body weight and energy metabolism in ovariectomized and estradiol-treated rats." Behav Neurosci **98**(4): 674-85.

Bezaire, V., L. L. Spriet, et al. (2005). "Constitutive UCP3 overexpression at physiological levels increases mouse skeletal muscle capacity for fatty acid transport and oxidation." Faseb J **19**(8): 977-9.

Blank, J. W. and S. D. Boggs (1993). "Successful treatment of an episode of malignant hyperthermia using a large dose of dantrolene." J Clin Anesth **5**(1): 69-72.

Boss, O., J. P. Giacobino, et al. (1998). "Genomic structure of uncoupling protein-3 (UCP3) and its assignment to chromosome 11q13." Genomics **47**(3): 425-6.

Boss, O., S. Samec, et al. (1998). "Uncoupling protein-3 expression in rodent skeletal muscle is modulated by food intake but not by changes in environmental temperature." J Biol Chem **273**(1): 5-8.

Boss, O., S. Samec, et al. (1997). "Uncoupling protein-3: a new member of the mitochondrial carrier family with tissue-specific expression." FEBS Lett **408**(1): 39-42.

Brand, M. D. and T. C. Esteves (2005). "Physiological functions of the mitochondrial uncoupling proteins UCP2 and UCP3." Cell Metab **2**(2): 85-93.

Brand, M. D., R. Pamplona, et al. (2002). "Oxidative damage and phospholipid fatty acyl composition in skeletal muscle mitochondria from mice underexpressing or overexpressing uncoupling protein 3." Biochem J **368**(Pt 2): 597-603.

Cadenas, S., J. A. Buckingham, et al. (1999). "UCP2 and UCP3 rise in starved rat skeletal muscle but mitochondrial proton conductance is unchanged." FEBS Lett **462**(3): 257-60.

Campbell, N. A. a. R., J.B. (2005). Biology, Pearson Education.

Cannon, B. and J. Nedergaard (2004). "Brown adipose tissue: function and physiological significance." Physiol Rev **84**(1): 277-359.

Casteilla, L., O. Champigny, et al. (1989). "Sequential changes in the expression of mitochondrial protein mRNA during the development of brown adipose tissue in bovine and ovine species. Sudden occurrence of uncoupling protein mRNA during embryogenesis and its disappearance after birth." Biochem J **257**(3): 665-71.

Chamberlain, P. D., K. H. Jennings, et al. (1999). "The tissue distribution of the human beta3-adrenoceptor studied using a monoclonal antibody: direct evidence of the beta3-

adrenoceptor in human adipose tissue, atrium and skeletal muscle." Int J Obes Relat Metab Disord **23**(10): 1057-65.
Chan, C. B. and M. E. Harper (2006). "Uncoupling proteins: role in insulin resistance and insulin insufficiency." Curr Diabetes Rev **2**(3): 271-83.
Choi, C. S., J. J. Fillmore, et al. (2007). "Overexpression of uncoupling protein 3 in skeletal muscle protects against fat-induced insulin resistance." J Clin Invest **117**(7): 1995-2003.
Coll, T., E. Eyre, et al. (2008). "Oleate reverses palmitate-induced insulin resistance and inflammation in skeletal muscle cells." J Biol Chem **283**(17): 11107-16.
Crabbe, J. C., J. K. Belknap, et al. (1994). "Quantitative trait loci mapping of genes that influence the sensitivity and tolerance to ethanol-induced hypothermia in BXD recombinant inbred mice." J Pharmacol Exp Ther **269**(1): 184-92.
Dulloo, A. G., S. Samec, et al. (2001). "Uncoupling protein 3 and fatty acid metabolism." Biochem Soc Trans **29**(Pt 6): 785-91.
Echtay, K. S., D. Roussel, et al. (2002). "Superoxide activates mitochondrial uncoupling proteins." Nature **415**(6867): 96-9.
Elgersma, Y., C. W. van Roermund, et al. (1995). "Peroxisomal and mitochondrial carnitine acetyltransferases of Saccharomyces cerevisiae are encoded by a single gene." Embo J **14**(14): 3472-9.
Feldmann, H. M., V. Golozoubova, et al. (2009). "UCP1 ablation induces obesity and abolishes diet-induced thermogenesis in mice exempt from thermal stress by living at thermoneutrality." Cell Metab **9**(2): 203-9.
Filppula, S. A., A. I. Yagi, et al. (1998). "Delta3,5-delta2,4-dienoyl-CoA isomerase from rat liver. Molecular characterization." J Biol Chem **273**(1): 349-55.
Flandin, P., Y. Donati, et al. (2005). "Hyperoxia-mediated oxidative stress increases expression of UCP3 mRNA and protein in skeletal muscle." FEBS Lett **579**(16): 3411-5.
Fleury, C., M. Neverova, et al. (1997). "Uncoupling protein-2: a novel gene linked to obesity and hyperinsulinemia." Nat Genet **15**(3): 269-72.
Foster, D. O., F. Depocas, et al. (1982). "Unilaterality of the sympathetic innervation of each pad of rat interscapular brown adipose tissue." Can J Physiol Pharmacol **60**(2): 107-13.
Foster, D. O. and M. L. Frydman (1978). "Nonshivering thermogenesis in the rat. II. Measurements of blood flow with microspheres point to brown adipose tissue as the dominant site of the calorigenesis induced by noradrenaline." Can J Physiol Pharmacol **56**(1): 110-22.
Freeman, H. C., A. Hugill, et al. (2006). "Deletion of nicotinamide nucleotide transhydrogenase: a new quantitive trait locus accounting for glucose intolerance in C57BL/6J mice." Diabetes **55**(7): 2153-6.
Gao, D., H. R. Griffiths, et al. (2009). "Oleate protects against palmitate-induced insulin resistance in L6 myotubes." Br J Nutr **102**(11): 1557-63.
Garlid, K. D., M. Jaburek, et al. (1998). "The mechanism of proton transport mediated by mitochondrial uncoupling proteins." FEBS Lett **438**(1-2): 10-4.
Golozoubova, V., E. Hohtola, et al. (2001). "Only UCP1 can mediate adaptive nonshivering thermogenesis in the cold." Faseb J **15**(11): 2048-50.
Gong, D. W., Y. He, et al. (1997). "Uncoupling protein-3 is a mediator of thermogenesis regulated by thyroid hormone, beta3-adrenergic agonists, and leptin." J Biol Chem **272**(39): 24129-32.

Gong, D. W., S. Monemdjou, et al. (2000). "Lack of obesity and normal response to fasting and thyroid hormone in mice lacking uncoupling protein-3." J Biol Chem **275**(21): 16251-7.
Gurvitz, A., A. M. Mursula, et al. (1999). "Alternatives to the isomerase-dependent pathway for the beta-oxidation of oleic acid are dispensable in Saccharomyces cerevisiae. Identification of YOR180c/DCI1 encoding peroxisomal delta(3,5)-delta(2,4)-dienoyl-CoA isomerase." J Biol Chem **274**(35): 24514-21.
Gurvitz, A., L. Wabnegger, et al. (1999). "Function of human mitochondrial 2,4-dienoyl-CoA reductase and rat monofunctional Delta3-Delta2-enoyl-CoA isomerase in beta-oxidation of unsaturated fatty acids." Biochem J **344 Pt 3**: 903-14.
Hagen, T. and B. B. Lowell (2000). "Chimeric proteins between UCP1 and UCP3: the middle third of UCP1 is necessary and sufficient for activation by fatty acids." Biochem Biophys Res Commun **276**(2): 642-8.
Harper, M. E., R. Dent, et al. (2002). "Decreased mitochondrial proton leak and reduced expression of uncoupling protein 3 in skeletal muscle of obese diet-resistant women." Diabetes **51**(8): 2459-66.
Hesselink, M. K. and P. Schrauwen (2005). "Towards comprehension of the physiological role of UCP3." Horm Metab Res **37**(9): 550-4.
Himms-Hagen, J. and M. E. Harper (1999). "Biochemical aspects of the uncoupling proteins: view from the chair." Int J Obes Relat Metab Disord **23 Suppl 6**: S30-2.
Himms-Hagen, J. and M. E. Harper (2001). "Physiological role of UCP3 may be export of fatty acids from mitochondria when fatty acid oxidation predominates: an hypothesis." Exp Biol Med (Maywood) **226**(2): 78-84.
Hittelman, K. J., O. Lindberg, et al. (1969). "Oxidative phosphorylation and compartmentation of fatty acid metabolism in brown fat mitochondria." Eur J Biochem **11**(1): 183-92.
Hsu, Y. H., T. Niu, et al. (2008). "Genetic variants in the UCP2-UCP3 gene cluster and risk of diabetes in the Women's Health Initiative Observational Study." Diabetes **57**(4): 1101-7.
Ito-Inaba, Y., Y. Hida, et al. (2008). "Molecular identity of uncoupling proteins in thermogenic skunk cabbage." Plant Cell Physiol **49**(12): 1911-6.
Jaburek, M. and K. D. Garlid (2003). "Reconstitution of recombinant uncoupling proteins: UCP1, -2, and -3 have similar affinities for ATP and are unaffected by coenzyme Q10." J Biol Chem **278**(28): 25825-31.
Jardine, D. S. (2007). "Heat illness and heat stroke." Pediatr Rev **28**(7): 249-58.
Jezek, P. (1999). "Fatty acid interaction with mitochondrial uncoupling proteins." J Bioenerg Biomembr **31**(5): 457-66.
Jezek, P. and E. Urbankova (2000). "Specific sequence of motifs of mitochondrial uncoupling proteins." IUBMB Life **49**(1): 63-70.
Jiang, N., G. Zhang, et al. (2009). "Upregulation of uncoupling protein-3 in skeletal muscle during exercise: a potential antioxidant function." Free Radic Biol Med **46**(2): 138-45.
Kim-Han, J. S., S. A. Reichert, et al. (2001). "BMCP1: a mitochondrial uncoupling protein in neurons which regulates mitochondrial function and oxidant production." J Neurochem **79**(3): 658-68.
Kozak, L. P. (2010). "Brown fat and the myth of diet-induced thermogenesis." Cell Metab **11**(4): 263-7.
Laloi, M., M. Klein, et al. (1997). "A plant cold-induced uncoupling protein." Nature **389**(6647): 135-6.

Larkin, S., E. Mull, et al. (1997). "Regulation of the third member of the uncoupling protein family, UCP3, by cold and thyroid hormone." Biochem Biophys Res Commun **240**(1): 222-7.
Lee, J. G., Y. J. Lee, et al. (2006). "Mutational and functional analysis of the cryptic N-terminal targeting signal for both mitochondria and peroxisomes in yeast peroxisomal citrate synthase Cit2p." J Biochem **140**(1): 121-33.
Liang, X., D. Zhu, et al. (1999). "Delta3,5,7,Delta2,4,6-trienoyl-CoA isomerase, a novel enzyme that functions in the beta-oxidation of polyunsaturated fatty acids with conjugated double bonds." J Biol Chem **274**(20): 13830-5.
Liebig, M., C. von Praun, et al. (2004). "Absence of UCP3 in brown adipose tissue does not impair nonshivering thermogenesis." Physiol Biochem Zool **77**(1): 116-26.
Liu, Y. J., P. Y. Liu, et al. (2005). "Linkage and association analyses of the UCP3 gene with obesity phenotypes in Caucasian families." Physiol Genomics **22**(2): 197-203.
Luthria, D. L., S. P. Baykousheva, et al. (1995). "Double bond removal from odd-numbered carbons during peroxisomal beta-oxidation of arachidonic acid requires both 2,4-dienoyl-CoA reductase and delta 3,5,delta 2,4-dienoyl-CoA isomerase." J Biol Chem **270**(23): 13771-6.
Major, G. C., E. Doucet, et al. (2007). "Clinical significance of adaptive thermogenesis." Int J Obes (Lond) **31**(2): 204-12.
Mao, G., G. A. Kraus, et al. "A mitochondria-targeted vitamin E derivative decreases hepatic oxidative stress and inhibits fat deposition in mice." J Nutr **140**(8): 1425-31.
Mao, W., X. X. Yu, et al. (1999). "UCP4, a novel brain-specific mitochondrial protein that reduces membrane potential in mammalian cells." FEBS Lett **443**(3): 326-30.
Mao, X., C. K. Kikani, et al. (2006). "APPL1 binds to adiponectin receptors and mediates adiponectin signalling and function." Nat Cell Biol **8**(5): 516-23.
Matthias, A., K. B. Ohlson, et al. (2000). "Thermogenic responses in brown fat cells are fully UCP1-dependent. UCP2 or UCP3 do not substitute for UCP1 in adrenergically or fatty scid-induced thermogenesis." J Biol Chem **275**(33): 25073-81.
McCoy, E. P., C. Renfrew, et al. (1994). "Malignant hyperpyrexia in an MDMA ("Ecstasy") abuser." Ulster Med J **63**(1): 103-7.
Mills, E. M., M. L. Banks, et al. (2003). "Pharmacology: uncoupling the agony from ecstasy." Nature **426**(6965): 403-4.
Modis, Y., S. A. Filppula, et al. (1998). "The crystal structure of dienoyl-CoA isomerase at 1.5 A resolution reveals the importance of aspartate and glutamate sidechains for catalysis." Structure **6**(8): 957-70.
Murphy, M. P., K. S. Echtay, et al. (2003). "Superoxide activates uncoupling proteins by generating carbon-centered radicals and initiating lipid peroxidation: studies using a mitochondria-targeted spin trap derived from alpha-phenyl-N-tert-butylnitrone." J Biol Chem **278**(49): 48534-45.
Nau, K., T. Fromme, et al. (2008). "Brown adipose tissue specific lack of uncoupling protein 3 is associated with impaired cold tolerance and reduced transcript levels of metabolic genes." J Comp Physiol B **178**(3): 269-77.
Nedergaard, J., T. Bengtsson, et al. (2007). "Unexpected evidence for active brown adipose tissue in adult humans." Am J Physiol Endocrinol Metab **293**(2): E444-52.

Nedergaard, J., V. Golozoubova, et al. (2001). "UCP1: the only protein able to mediate adaptive non-shivering thermogenesis and metabolic inefficiency." Biochim Biophys Acta **1504**(1): 82-106.

Nedergaard, J., A. Matthias, et al. (1999). "UCP1: the original uncoupling protein--and perhaps the only one? New perspectives on UCP1, UCP2, and UCP3 in the light of the bioenergetics of the UCP1-ablated mice." J Bioenerg Biomembr **31**(5): 475-91.

Nicholls, D. G. (1976). "Hamster brown-adipose-tissue mitochondria. Purine nucleotide control of the ion conductance of the inner membrane, the nature of the nucleotide binding site." Eur J Biochem **62**(2): 223-8.

Ojima, K., A. Uezumi, et al. (2004). "Mac-1(low) early myeloid cells in the bone marrow-derived SP fraction migrate into injured skeletal muscle and participate in muscle regeneration." Biochem Biophys Res Commun **321**(4): 1050-61.

Palmieri, F. (2004). "The mitochondrial transporter family (SLC25): physiological and pathological implications." Pflugers Arch **447**(5): 689-709.

Petrovic, N., G. Cvijic, et al. (2003). "Thyroxine and tri-iodothyronine differently affect uncoupling protein-1 content and antioxidant enzyme activities in rat interscapular brown adipose tissue." J Endocrinol **176**(1): 31-8.

Pierrat, B., M. Ito, et al. (2000). "Uncoupling proteins 2 and 3 interact with members of the 14.3.3 family." Eur J Biochem **267**(9): 2680-7.

Rafael, J., H. J. Ludolph, et al. (1969). "[Mitochondria from brown adipose tissue: uncoupling of respiratory chain phosphorylation by long fatty acids and recoupling by guanosine triphosphate]." Hoppe Seylers Z Physiol Chem **350**(9): 1121-31.

Ren, Y., J. Aguirre, et al. (2004). "An alternative pathway of oleate beta-oxidation in Escherichia coli involving the hydrolysis of a dead end intermediate by a thioesterase." J Biol Chem **279**(12): 11042-50.

Ren, Y. and H. Schulz (2003). "Metabolic functions of the two pathways of oleate beta-oxidation double bond metabolism during the beta-oxidation of oleic acid in rat heart mitochondria." J Biol Chem **278**(1): 111-6.

Roberts, J. C. and R. E. Smith (1967). "Time-dependent responses of brown fat in cold-exposed rats." Am J Physiol **212**(2): 519-25.

Rothwell, N. J. and M. J. Stock (1979). "A role for brown adipose tissue in diet-induced thermogenesis." Nature **281**(5726): 31-5.

Rothwell, N. J. and M. J. Stock (1984). "Tissue blood flow in control and cold-adapted hyperthyroid rats." Can J Physiol Pharmacol **62**(8): 928-33.

Rusyniak, D. E., M. L. Banks, et al. (2004). "Dantrolene use in 3,4-methylenedioxymethamphetamine (ecstasy)-mediated hyperthermia." Anesthesiology **101**(1): 263; author reply 264.

Rusyniak, D. E., Y. Ootsuka, et al. (2008). "When administered to rats in a cold environment, 3,4-methylenedioxymethamphetamine reduces brown adipose tissue thermogenesis and increases tail blood flow: effects of pretreatment with 5-HT1A and dopamine D2 antagonists." Neuroscience **154**(4): 1619-26.

Rusyniak, D. E., S. L. Tandy, et al. (2005). "The role of mitochondrial uncoupling in 3,4-methylenedioxymethamphetamine-mediated skeletal muscle hyperthermia and rhabdomyolysis." J Pharmacol Exp Ther **313**(2): 629-39.

Samec, S., J. Seydoux, et al. (1998). "Role of UCP homologues in skeletal muscles and brown adipose tissue: mediators of thermogenesis or regulators of lipids as fuel substrate?" Faseb J **12**(9): 715-24.
Schrauwen, P. and M. K. Hesselink (2004). "The role of uncoupling protein 3 in fatty acid metabolism: protection against lipotoxicity?" Proc Nutr Soc **63**(2): 287-92.
Schrauwen, P., M. K. Hesselink, et al. (2002). "Effect of acute exercise on uncoupling protein 3 is a fat metabolism-mediated effect." Am J Physiol Endocrinol Metab **282**(1): E11-7.
Schrauwen, P., J. Hoeks, et al. (2006). "Putative function and physiological relevance of the mitochondrial uncoupling protein-3: involvement in fatty acid metabolism?" Prog Lipid Res **45**(1): 17-41.
Schrauwen, P., M. Mensink, et al. (2006). "Reduced skeletal muscle uncoupling protein-3 content in prediabetic subjects and type 2 diabetic patients: restoration by rosiglitazone treatment." J Clin Endocrinol Metab **91**(4): 1520-5.
Schrauwen, P., J. Xia, et al. (1999). "Skeletal muscle uncoupling protein 3 expression is a determinant of energy expenditure in Pima Indians." Diabetes **48**(1): 146-9.
Schrauwen, P., J. Xia, et al. (1999). "A novel polymorphism in the proximal UCP3 promoter region: effect on skeletal muscle UCP3 mRNA expression and obesity in male non-diabetic Pima Indians." Int J Obes Relat Metab Disord **23**(12): 1242-5.
Seifert, E. L., V. Bezaire, et al. (2008). "Essential role for uncoupling protein-3 in mitochondrial adaptation to fasting but not in fatty acid oxidation or fatty acid anion export." J Biol Chem **283**(37): 25124-31.
Shoukry, K. and H. Schulz (1998). "Significance of the reductase-dependent pathway for the beta-oxidation of unsaturated fatty acids with odd-numbered double bonds. Mitochondrial metabolism of 2-trans-5-cis-octadienoyl-CoA." J Biol Chem **273**(12): 6892-9.
Shyu, Y. J., H. Liu, et al. (2006). "Identification of new fluorescent protein fragments for bimolecular fluorescence complementation analysis under physiological conditions." Biotechniques **40**(1): 61-6.
Skulachev, V. P. (1999). "Anion carriers in fatty acid-mediated physiological uncoupling." J Bioenerg Biomembr **31**(5): 431-45.
Smith, A. M., R. G. Ratcliffe, et al. (2004). "Activation and function of mitochondrial uncoupling protein in plants." J Biol Chem **279**(50): 51944-52.
Smith, R. E. and R. J. Hock (1963). "Brown fat: thermogenic effector of arousal in hibernators." Science **140**: 199-200.
Smith, R. E. and B. A. Horwitz (1969). "Brown fat and thermogenesis." Physiol Rev **49**(2): 330-425.
Son, C., K. Hosoda, et al. (2004). "Reduction of diet-induced obesity in transgenic mice overexpressing uncoupling protein 3 in skeletal muscle." Diabetologia **47**(1): 47-54.
Sprague, J. E., M. L. Banks, et al. (2003). "Hypothalamic-pituitary-thyroid axis and sympathetic nervous system involvement in hyperthermia induced by 3,4-methylenedioxymethamphetamine (Ecstasy)." J Pharmacol Exp Ther **305**(1): 159-66.
Sprague, J. E., N. M. Mallett, et al. (2004). "UCP3 and thyroid hormone involvement in methamphetamine-induced hyperthermia." Biochem Pharmacol **68**(7): 1339-43.

Sprague, J. E., P. Moze, et al. (2005). "Carvedilol reverses hyperthermia and attenuates rhabdomyolysis induced by 3,4-methylenedioxymethamphetamine (MDMA, Ecstasy) in an animal model." Crit Care Med **33**(6): 1311-6.

Sprague, J. E., X. Yang, et al. (2007). "Roles of norepinephrine, free Fatty acids, thyroid status, and skeletal muscle uncoupling protein 3 expression in sympathomimetic-induced thermogenesis." J Pharmacol Exp Ther **320**(1): 274-80.

Stuart, J. A., J. A. Harper, et al. (1999). "Uncoupling protein 2 from carp and zebrafish, ectothermic vertebrates." Biochim Biophys Acta **1413**(1): 50-4.

Talbot, D. A., N. Hanuise, et al. (2003). "Superoxide activates a GDP-sensitive proton conductance in skeletal muscle mitochondria from king penguin (Aptenodytes patagonicus)." Biochem Biophys Res Commun **312**(4): 983-8.

Talbot, D. A., A. J. Lambert, et al. (2004). "Production of endogenous matrix superoxide from mitochondrial complex I leads to activation of uncoupling protein 3." FEBS Lett **556**(1-3): 111-5.

Thompson, M. P. and D. Kim (2004). "Links between fatty acids and expression of UCP2 and UCP3 mRNAs." FEBS Lett **568**(1-3): 4-9.

Van Gilst, M. R., H. Hadjivassiliou, et al. (2005). "Nuclear hormone receptor NHR-49 controls fat consumption and fatty acid composition in C. elegans." PLoS Biol **3**(2): e53.

Vidal-Puig, A., G. Solanes, et al. (1997). "UCP3: an uncoupling protein homologue expressed preferentially and abundantly in skeletal muscle and brown adipose tissue." Biochem Biophys Res Commun **235**(1): 79-82.

Vidal-Puig, A. J., D. Grujic, et al. (2000). "Energy metabolism in uncoupling protein 3 gene knockout mice." J Biol Chem **275**(21): 16258-66.

Weigert, C., K. Brodbeck, et al. (2004). "Palmitate, but not unsaturated fatty acids, induces the expression of interleukin-6 in human myotubes through proteasome-dependent activation of nuclear factor-kappaB." J Biol Chem **279**(23): 23942-52.

Whatcott, C. J., M. L. Meyer-Ficca, et al. (2009). "A specific isoform of poly(ADP-ribose) glycohydrolase is targeted to the mitochondrial matrix by a N-terminal mitochondrial targeting sequence." Exp Cell Res **315**(20): 3477-85.

Zackova, M., E. Skobisova, et al. (2003). "Activating omega-6 polyunsaturated fatty acids and inhibitory purine nucleotides are high affinity ligands for novel mitochondrial uncoupling proteins UCP2 and UCP3." J Biol Chem **278**(23): 20761-9.

Zhang, D., X. Liang, et al. (2001). "Delta 3,5,delta 2,4-dienoyl-CoA isomerase is a multifunctional isomerase. A structural and mechanistic study." J Biol Chem **276**(17): 13622-7.

Zingaretti, M. C., F. Crosta, et al. (2009). "The presence of UCP1 demonstrates that metabolically active adipose tissue in the neck of adult humans truly represents brown adipose tissue." Faseb J **23**(9): 3113-20.

Vita

Monte Alexander (Alex) Kenaston was born in Memphis, Tennessee on September 8th 1976, the youngest son of Monte and Maria Kenaston. After graduating from Lausanne Collegiate School (Memphis, TN) in 1994, he attended the University of Texas at Austin and received a Bachelor of Science in Nursing in 1998. Following graduation he worked in trauma/spinal nursing at Brackenridge Hospital (Austin, TX) for 2.5 years, then began pursing clinical research with Pharmaceutical Product Development, Inc (Austin, TX). In 2005 he joined the graduate school in the College of Pharmacy at the University of Texas at Austin under the tutelage of Dr. Edward M. Mills.

Permanent address: 105 Spur Cove, Kyle, TX 78640 USA

This dissertation was typed by the author.